J

EFFECT OF THE RING CURRENT ON

THE DISTRIBUTION OF UNBOUND

PARTICLES IN THE MAGNETOSPHERE

by Perry F. McDonald

June 1966

RESEARCH LABORATORIES

BROWN ENGINEERING COMPANY, INC.

HUNTSVILLE, ALABAMA

TECHNICAL NOTE R-204

EFFECT OF THE RING CURRENT ON THE DISTRIBUTION
OF UNBOUND PARTICLES IN THE MAGNETOSPHERE

June 1966

Prepared For

NUCLEAR AND PLASMA PHYSICS BRANCH
RESEARCH PROJECTS LABORATORY
GEORGE C. MARSHALL SPACE FLIGHT CENTER

Prepared By

RESEARCH LABORATORIES
BROWN ENGINEERING COMPANY, INC.

Contract No. NAS8-20166

Prepared By

Perry F. McDonald
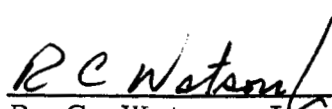
ABSTRACT

12234

The effect of the ring current due to the drift of trapped particles in the radiation belts on the distribution of untrapped particles in the magnetosphere is analyzed using a current sheet approximation to the ring current. The shape assumed for the current sheet is the figure obtained by rotating a dipole field line about the axis. The vector potential of a dipole plus a distributed ring current is derived and applied in Störmer's theorem to determine allowed and forbidden regions of particle motion. Liouville's theorem is used to obtain the ratio of unbound particle flux at points inside the model magnetosphere to an isotropic uniform flux at infinity.

Author

Approved:

J. E. White, Jr.
Research Projects Coordinator

Approved:

R. C. Watson, Jr.
Vice President
Advanced Systems & Technologies

TABLE OF CONTENTS

LIST OF FIGURES

LIST OF FIGURES (Continued)

LIST OF SYMBOLS

$\vec{A}$	Vector potential
A_ϕ	The ϕ component of $\vec{A}$
a	Radius of the current sheet at the equator
b	Radial distance to circular current loop
C_{in}	Expansion coefficients for central field vector potential
C_{on}	Expansion coefficients for the remote field vector potential
C_{st}	Störmer unit of length
E	Energy
$F(\beta)$	Defined by Equation 16
$f(\vec{r}, \vec{p})$, $f(\vec{r}, \vec{P})$	Distribution function
I	Current
j	Current density per unit length along the current sheet
ℓ	Coordinate along an arc of current sheet
M	Magnetic moment of geomagnetic dipole
M_R	Magnetic moment of sheet current
n	Dummy index
$\vec{P}$	$\vec{p} + q\vec{A}$
$P_n^1(\cos\theta)$	Associated Legendre polynomial
p	$\lvert\vec{p}\rvert$
$\vec{p}$	Particle momentum
Q	Defined by Equation 17
q	Particle charge (positive)

R	Radius in cylindrical polar coordinates
(r, θ, ϕ)	Spherical coordinates at a field point
(r', ψ, θ)	Spherical coordinates of source point on current sheet
$\vec{r}$	Radius vector
$\vec{r}_\infty$	Point at infinity
$\vec{v}$	Particle velocity
v	$|\vec{v}|$
$\vec{v}_E$	Speed corresponding to energy E
α	$\equiv \beta$ for $r < a \sin^2 \beta$
α	$\equiv \sin^{-1}\left(\dfrac{r}{a}\right)^{\frac{1}{2}}$ for $a \sin^2 \beta < r < a$
α	$\equiv \dfrac{\pi}{2}$ $r > a$
β	Value of θ where j becomes zero
γ	Impact parameter
$\bar{\gamma}$	γ / C_{st}
λ	a / C_{st}
μ	Permeability (mks units)
ρ	r / C_{st}
$\Phi(\vec{r}, E)$	Flux at point r of particles with energy E
Ω	Solid angle

INTRODUCTION

A westward flowing equatorial ring current was first proposed by Schmidt[1] to explain the decrease in the horizontal component of the magnetic field at the Earth's surface during magnetic storms. Chapman and Ferraro[2] proposed that charged particle streams from the Sun provide the source for the ring current. They also speculated that a westward flowing ring current at the geomagnetic equator with a radius between five and ten Earth radii might serve as a reservoir of particles to produce the auroras as well as explain the decrease in the Earth's field during the main phase of geomagnetic storms. The annular current causing a decrease was not attributed to the drift of charged particles trapped in the geomagnetic field but to a charge distribution of particles of the neutral solar flux on the boundary of the magnetosphere. Alfvén[3] showed that magnetic traps can exist in the Earth's dipole field and that these traps correspond to Störmer's inner allowed region. The radiation belts provide a collection of charged particles whose drift causes a ring current.

Treiman[4] assumed a ring current formed by a current sheet located on the surface of a sphere concentric with the Earth and obtained an expression for the variation expected in the intensity of cosmic radiation near the Earth's surface. Ray[5] assumed a filamentary form for the equatorial ring current and determined the allowed and forbidden regions of particle motion using Störmer's theory. The effect of the ring current on the vertical cutoff rigidity at the Earth's surface was studied as a function of geomagnetic latitude. Ray[6] also studied the effect of the ring current on the impact zones of cosmic rays by integrating particle trajectories. There has been some difficulty in reconciling the measured particle population and calculated ring current with the observed reduction in cosmic ray cutoff rigidity during magnetic storms[7].

In this paper the ring current due to the drift of charged particles trapped in the radiation belts is approximated by a single current sheet

symmetric about the dipole axis and with cross-sectional shape like that of a dipole field line.

The vector potential for the combination of the geomagnetic dipole and the distributed ring current is expanded in terms of the associated Legendre polynomials and inserted into Störmer's theorem. Störmer's theorem is used to determine the allowed and forbidden regions for motion of untrapped particles. Finally, Liouville's theorem is used to determine the ratio of the proton flux for selected energies at points inside the magnetosphere to the flux of protons of the same energy at infinity. The flux is assumed to be isotropic and spatially uniform at infinity.

AN APPROXIMATION TO THE VECTOR POTENTIAL
OF THE RADIATION BELTS

Approximations to the ring current field have been studied by Akasofu and Cain[8,9], Akasofu and Chapman[10], Ben'kova and Tyurmina[11], Chapman[12], and Ray[13]. Ben'kova and Tyurmina have studied the potential of a current sheet, the surface of which is generated by rotating a dipole field line about the dipole axis. The ring current is due to the drift of particles trapped in the radiation belts by the Earth's magnetic field which is largely that of a dipole over a substantial part of the magnetosphere. The approximation of the current distribution by a sheet of the general shape of the radiation belts seems reasonable and should be more representative of nature than a filamentary ring current.

The shape of a dipole field line is given by

$$r' = a \sin^2 \psi$$

where a is the value of r in the equatorial plane and ψ is the magnetic colatitude of a point on the current surface (see Figure 1). The current's surface is assumed to be axisymmetric and symmetric with respect to the equatorial plane and the current is assumed to diminish to zero at some $\psi = \beta$ and $\psi = \pi - \beta$. The current is assumed to flow along the surface from east to west and it is assumed that the r and θ components of the current are zero.

The vector potential of a circular loop at r = b and $\theta = \psi$ is given by Smythe[14] in terms of the associated Legendre polynomials for r < b,

$$\vec{A} = \hat{\phi} \frac{\mu I}{2} \sum_{n=1}^{\infty} \frac{\sin \psi}{n(n+1)} \left(\frac{r}{b}\right)^n P_n^1 (\cos \psi) P_n^1 (\cos \theta) \tag{1a}$$

and for r > b,

$$\vec{A} = \hat{\phi} \frac{\mu I}{2} \sum_{n=1}^{\infty} \frac{\sin \psi}{n(n+1)} \left(\frac{b}{r}\right)^{n+1} P_n^1 (\cos \psi) P_n^1 (\cos \theta) \tag{1b}$$

3
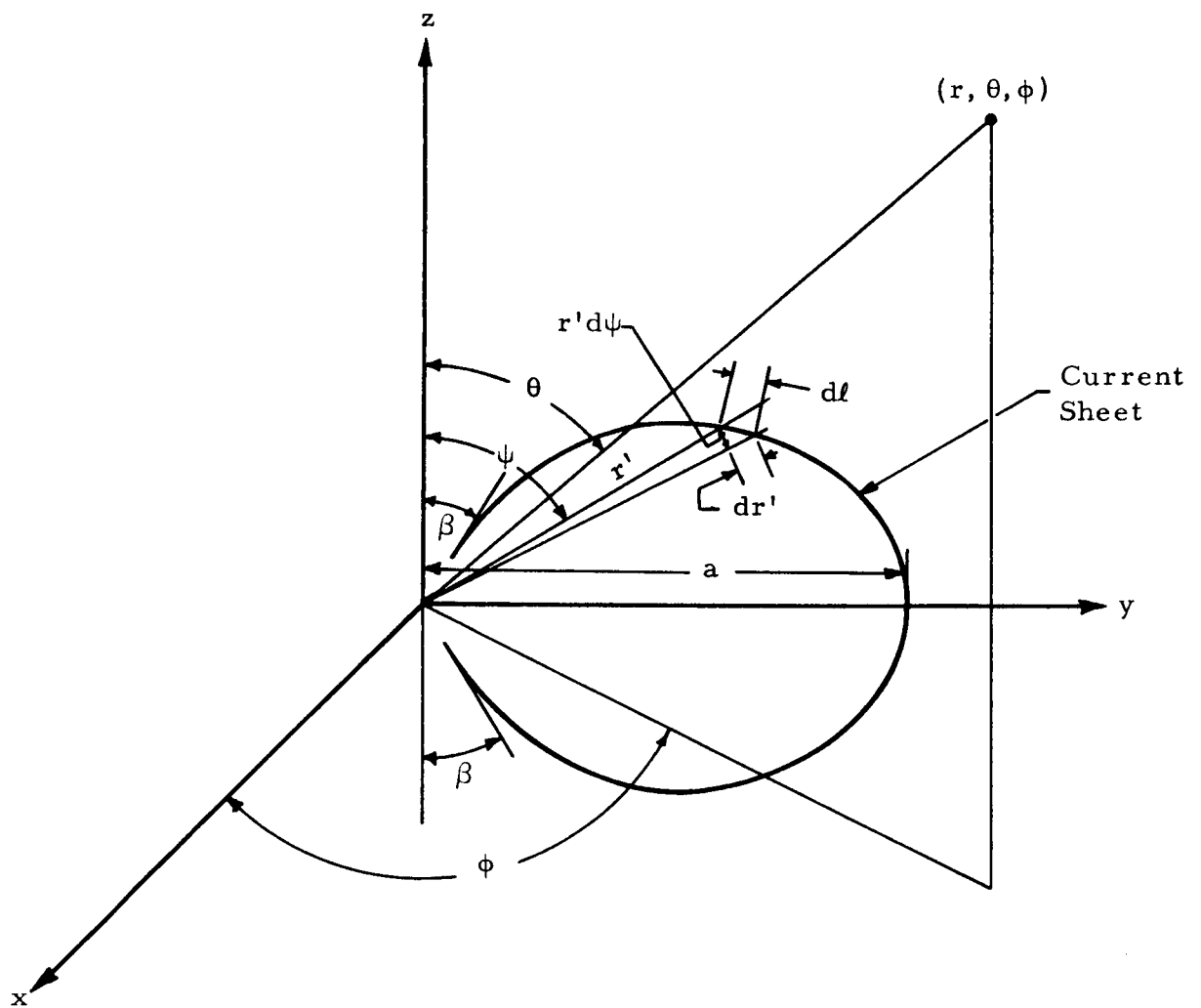
Figure 1. Coordinates of the Current Sheet and Field Point

where μ is the permeability and I is the current. The vector potential of such a circular loop has a ϕ component only. The current sheet can be thought of as being composed of a large number of circular current belts with very small widths. The vector potential at a field point (r, θ) of one of these belts located at (r', ψ) may be represented by

$$dA_\phi = \mu \frac{dI}{2} \sum_{n=1}^{\infty} \frac{\sin \psi}{n(n+1)} \left(\frac{r}{r'}\right)^n P_n^1 (\cos \psi) \, P_n^1 (\cos \theta) \qquad (2a)$$

if $r < r'$, or by

$$dA_\phi = \mu \frac{dI}{2} \sum_{n=1}^{\infty} \frac{\sin \psi}{n(n+1)} \left(\frac{r'}{r}\right)^{n+1} P_n^1 (\cos \psi) \, P_n^1 (\cos \theta) \qquad (2b)$$

if $r > r'$.

The current, dI, in a very narrow belt of width $d\ell$ is given by

$$dI = j \, d\ell$$

where j is the current density per unit arc length along the current sheet. The current density is assumed to be a function of ψ, $j = j(\psi)$.

The vector potential, A_ϕ, of the sheet can be found by integrating Equations 2 along a line of force of the magnetic field.

$$A_\phi = \int_{S_1}^{S_2} dA_\phi = \frac{\mu}{2} \int_{S_1}^{S_2} j \sum_{n=1}^{\infty} \frac{\sin \psi}{n(n+1)} \left(\frac{r}{r'}\right)^n P_n^1 (\cos \psi) \, P_n^1 (\cos \theta) \, d\ell \qquad (3a)$$

if $r < r'$ or

$$A_\phi = \frac{\mu}{2} \int_{S_3}^{S_4} j \sum_{n=1}^{\infty} \frac{\sin \psi}{n(n+1)} \left(\frac{r'}{r}\right)^{n+1} P_n^1 (\cos \psi) \, P_n^1 (\cos \theta) \, d\ell \qquad (3b)$$

if $r > r'$, where S_1, S_2, S_3, and S_4 are points on the sheet of current.

5

Integration is along an arc of the curve

$$r' = a \sin^2 \psi \quad . \tag{4}$$

The computations are facilitated by replacing the integration along the arc ℓ by integration over the angle ψ. From Figure 1 it is evident that

$$(d\ell)^2 = (dr')^2 + (r' d\psi)^2$$

but $dr' = 2 a \sin \psi \cos \psi \, d\psi$, and

$$d\ell = a \sin \psi (1 + 3 \cos^2 \psi)^{\frac{1}{2}} d\psi \quad . \tag{5}$$

Making this substitution one obtains

$$A_\phi = \frac{a\mu}{2} \int_\beta^{\pi-\beta} j \sum_{n=1}^\infty \frac{\sin^2 \psi}{n(n+1)} \left(\frac{r}{a \sin^2 \psi}\right)^n P_n^1 (\cos \psi) \, P_n^1 (\cos \theta)$$

$$\times (1 + 3 \cos^2 \psi)^{\frac{1}{2}} d\psi \tag{6a}$$

if $r < a \sin^2 \beta$, or by

$$A_\phi = \frac{a\mu}{2} \int_\beta^{\pi-\beta} j \sum_{n=1}^\infty \frac{\sin^2 \psi}{n(n+1)} \left(\frac{a \sin^2 \psi}{r}\right)^{n+1} P_n^1 (\cos \psi) \, P_n^1 (\cos \theta)$$

$$\times (1 + 3 \cos^2 \psi)^{\frac{1}{2}} d\psi \tag{6b}$$

if $r > a$. These integrals converge in the regions specified. In the region $a \sin^2 \beta < r < a$, the vector potential is the sum of a central and a remote field contribution. If the field point is (r, θ), then the central field contribution can be evaluated by integrating over the current which is distributed at $r' > r$. The remote field contribution is evaluated by integrating over the current which is distributed at $r' < r$. These integrals will converge provided j is bounded. The vector potential in this intermediate range is given by

6

$$A_\phi = A_{\phi i} + A_{\phi o} \quad \text{for} \quad a \sin^2 \beta < r < a \tag{7}$$

where $A_{\phi i}$ is the central field contribution and $A_{\phi o}$ is the remote field contribution (see Figure 2).

$$A_{\phi i} = \frac{a\mu}{2} \int_\alpha^{\pi-\alpha} j \sum_{n=1}^\infty \frac{\sin^2 \psi}{n(n+1)} \left(\frac{r}{a \sin^2 \psi} \right)^n P_n^1 (\cos \psi) \, P_n^1 (\cos \theta)$$

$$\times (1 + 3 \cos^2 \psi)^{\frac{1}{2}} \, d\psi \tag{8}$$

where $\alpha = \sin^{-1} (r/a)^{\frac{1}{2}}$ and $a \sin^2 \beta < r < a$.

$$A_{\phi o} = \frac{a\mu}{2} \int_\beta^{\pi-\beta} j \sum_{n=1}^\infty \frac{\sin^2 \psi}{n(n+1)} \left(\frac{a \sin^2 \psi}{r} \right)^{n+1} P_n^1 (\cos \psi) \, P_n^1 (\cos \theta) (1 + 3 \cos^2 \psi)^{\frac{1}{2}} \, d\psi$$

$$- \frac{a\mu}{2} \int_\alpha^{\pi-\alpha} j \sum_{n=1}^\infty \frac{\sin^2 \psi}{n(n+1)} \left(\frac{a \sin^2 \psi}{r} \right)^{n+1} P_n^1 (\cos \psi) \, P_n^1 (\cos \theta) (1 + 3 \cos^2 \psi)^{\frac{1}{2}} \, d\psi$$

$$\tag{9}$$

It is necessary to assume a form for j before proceeding to evaluate the integrals. Ben'kova and Tyurmina[11] considered several different functional dependences of j on ψ, but for this study it was assumed that $j = j_o \sin^2 \psi$ where j_o is a constant. With this assumption, the vector potential becomes

$$A_\phi = \frac{a\mu j_o}{2} \sum_{n=1}^\infty \frac{1}{n(n+1)} \left\{ \left(\frac{r}{a} \right)^n C_{in}(\alpha) + \left(\frac{a}{r} \right)^{n+1} \left[C_{on}(\beta) - C_{on}(\alpha) \right] \right\} P_n^1 (\cos \theta) \tag{10}$$

where

$$C_{in}(\alpha) = \int_\alpha^{\pi-\alpha} \frac{P_n^1 (\cos \psi)}{(\sin \psi)^{2n-4}} (1 + 3 \cos^2 \psi)^{\frac{1}{2}} \, d\psi \quad , \tag{11a}$$

7
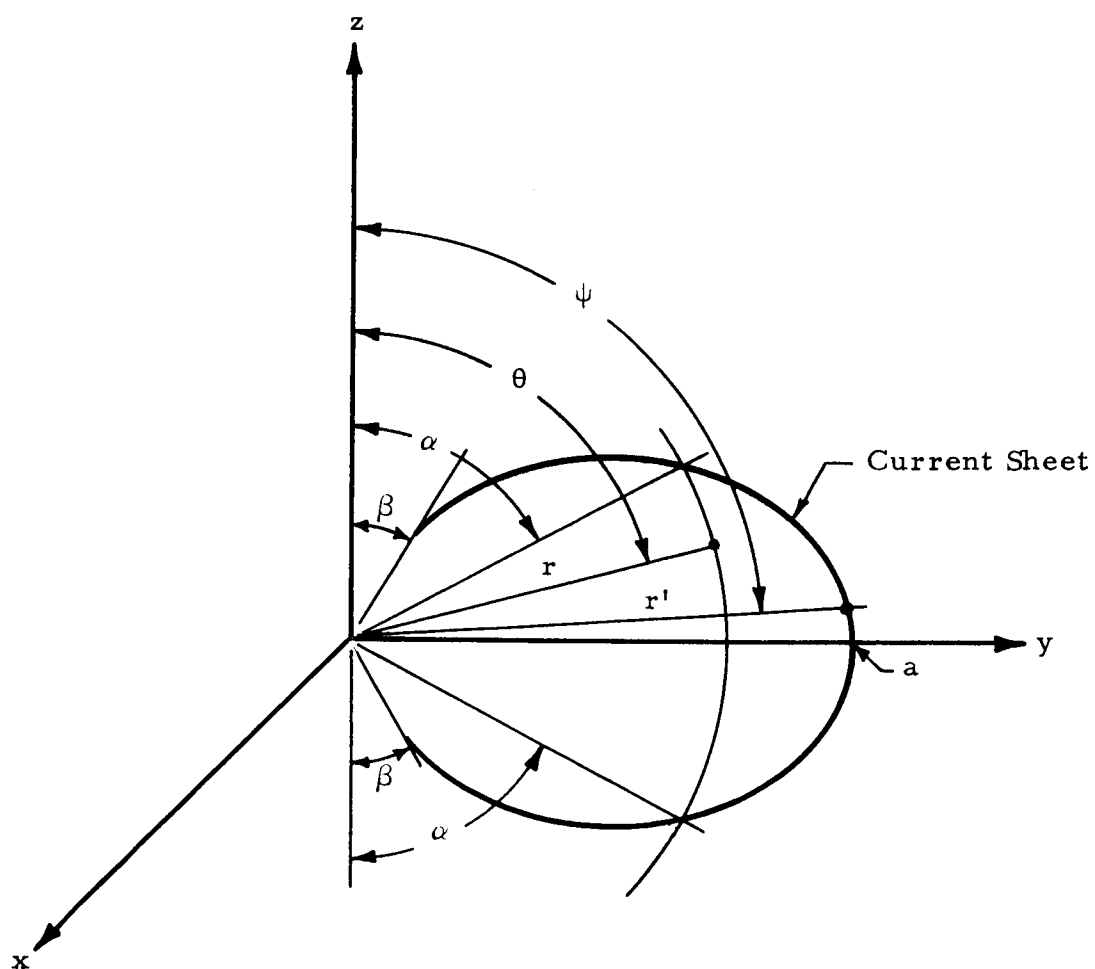
Figure 2. Coordinates for Intermediate
Vector Potential Calculations

$$C_{on}(\alpha) = \int_{\alpha}^{\pi-\alpha} (\sin \psi)^{2n+6} \, P_n^1 (\cos \psi) \, (1 + 3 \cos^2 \psi)^{\frac{1}{2}} \, d\psi \qquad (11b)$$

$$\alpha \equiv \beta \quad \text{for} \quad r < a \sin^2 \beta$$

and

$$\alpha \equiv \pi/2 \quad \text{for} \quad r > a \quad .$$

These integrals can be evaluated by expanding the associated Legendre polynomials in terms of $\sin \psi$ and using a set of integral tables such as that of Gröbner and Hofreiter[15]. The integrals are tedious to evaluate by hand but a computer may be used to construct a table of evaluated integrals and the coefficients are linear combinations of elements of the table.

MAGNETIC MOMENT

The magnetic moment of a current loop carrying current dI is

$$dM = \pi R^2 dI$$

where R is the radius of the loop. From Equations 4 and 5

$$R = a \sin^3 \psi$$

and

$$dI = j \, d\ell = j \, a \sin \psi \, (1 + 3 \cos^2 \psi)^{\frac{1}{2}} \, d\psi$$

one obtains

$$dM_R = \pi \, a^3 \, j \sin^7 \psi \, (1 + 3 \cos^2 \psi)^{\frac{1}{2}} \, d\psi \tag{12}$$

and the magnetic moment[11] of the sheet is given by

$$M_R = \int_{Sheet} dM_R$$

or

$$M_R = \pi \, a^3 \int_{\beta}^{\pi - \beta} j \sin^7 \psi \, (1 + 3 \cos^2 \psi)^{\frac{1}{2}} \, d\psi \quad . \tag{13}$$

If a current distribution of the form $j = j_0 \sin^2 \psi$ is assumed, then

$$M_R = \pi \, j_0 \, a^3 \, F(\beta) \quad , \tag{14}$$

or

$$j_0 = \frac{M_R}{\pi \, a^3 \, F(\beta)} \tag{15}$$

where

$$F(\beta) \equiv \int_{\beta}^{\pi - \beta} \sin^9 \psi \, (1 + 3 \cos^2 \psi)^{\frac{1}{2}} \, d\psi \quad . \tag{16}$$

STÖRMER'S THEOREM FOR A DIPOLE PLUS
A DISTRIBUTED RING CURRENT

Störmer's theorem for charged particle motion in axisymmetric magnetic fields is written (Stern[16])

$$Q = \cos \omega = -\frac{v_\phi}{v} = \frac{q}{p} A_\phi + \frac{2\gamma}{r \sin \theta} \tag{17}$$

where v_ϕ is the ϕ component of velocity, v is the magnitude of particle velocity, q and p are the charge and momentum of the particle, γ is the impact parameter and ω is the angle between $\vec{V}$ and west.

The vector potential of a dipole plus the distributed ring current being considered is, using Equations 10, 11, and 15,

$$A_\phi = \frac{\mu_0 \, M \sin \theta}{4\pi \, r^2} + \frac{\mu_0 \, M_R}{2\pi \, a^2 \, F(\beta)} \left(\sum_{n=1}^{\infty} \frac{1}{n(n+1)} \left\{ \left(\frac{r}{a}\right)^n C_{in}(\alpha) \right. \right.$$

$$\left. \left. + \left(\frac{a}{r}\right)^{n+1} [C_{on}(\beta) - C_{on}(\alpha)] \right\} P_n^1 (\cos \theta) \right) \tag{18}$$

where M is the magnetic moment of the dipole. Substituting Equation 18 into Equation 17 yields

$$Q = \frac{q \, \mu_0 \, M \sin \theta}{4p \, \pi \, r^2} + \frac{q \, \mu_0 \, M_R}{2\pi \, p \, a^2 \, F(\beta)} \sum_{n=1}^{\infty} \frac{1}{n(n+1)} \left\{ \left(\frac{r}{a}\right)^n C_{in}(\alpha) \right.$$

$$\left. + \left(\frac{a}{r}\right)^{n+1} [C_{on}(\beta) - C_{on}(\alpha)] \right\} P_n^1 (\cos \theta) + \frac{2\gamma}{r \sin \theta} \quad . \tag{19}$$

The Störmer unit of length is defined to be

$$C_{st}^{\,2} \equiv \frac{q \, \mu_0 \, M}{4\pi \, p} \tag{20}$$

13

and Equation 19 may be made dimensionless using the definitions $\rho \equiv r/C_{st}$, $\lambda \equiv a/C_{st}$ and $\bar{\gamma} \equiv \gamma/C_{st}$. When these substitutions are made, one obtains

$$Q = \frac{\sin \theta}{\rho^2} + \frac{2\bar{\gamma}}{\rho \sin \theta} + \frac{2 M_R}{M \lambda^2 F(\beta)} \sum_{n=1}^{\infty} \frac{1}{n(n+1)} \left\{ \left(\frac{\rho}{\lambda}\right)^n C_{in}(\alpha) \right.$$

$$\left. + \left(\frac{\lambda}{\rho}\right)^{n+1} [C_{on}(\beta) - C_{on}(\alpha)] \right\} P_n^1 (\cos \theta) \quad . \quad (21)$$

The application of Störmer's theorem to the dipole shielding problem has been discussed in detail by Störmer[17], Vallarta[18], Johnson[19] and Ray[5]. Störmer's theorem for more complex field configurations such as double ring currents and multipole fields has been analyzed in detail by Urban[20, 21] and Prescott[22, 23].

Equation 21 contains four free parameters, three of which describe the current sheet (M_R/M, λ and β) and $\bar{\gamma}$ which is the normalized impact parameter of the particle. Since Q is the cosine of the angle between the particle's velocity vector and west, Equation 21 can only describe real particle motion for $|Q| \leq 1$. Allowed and forbidden regions comparable to those shown, for example, by Ray[5] and Urban[21] may be found from this equation.

SADDLE POINTS IN THE Q SURFACE

The hypersurface Q (ρ, θ, λ, β, $\overline{\gamma}$, M_R/M) may be analyzed for saddle points where $Q = -1$. Saddle points in the Q surface and their significance have been discussed in detail by Urban[20, 21] and by Prescott[22, 23]. Location of saddle points in the Q surface leads to the determination of totally shielded, partially shielded and unshielded regions of Störmer space and permits calculation of the normalized particle flux (relative to an isotropic distribution at infinity) in the partially shielded regions.

In order for a saddle point to exist for a function $F(\rho, \theta)$ at a given point, the following conditions must be satisfied at that point:

$$\frac{\partial F}{\partial \rho} = 0, \quad \frac{1}{\rho} \frac{\partial F}{\partial \theta} = 0 \tag{22}$$

and

$$\left(\frac{1}{\rho} \frac{\partial^2 F}{\partial \rho \, \partial \theta}\right)^2 - \left(\frac{\partial^2 F}{\partial \rho^2}\right)\left(\frac{1}{\rho^2} \frac{\partial^2 F}{\partial \theta^2}\right) > 0 \quad . \tag{23}$$

Equation 22 is the necessary condition and Equation 23 is the sufficient condition.

Application of Equation 22 to Equation 21 yields the results

$$\frac{\partial Q}{\partial \rho} = 0 = -\frac{2 \sin \theta}{\rho_c^{\,3}} \frac{-2 \, \overline{\gamma}_c}{\rho_c^2 \sin \theta} + \frac{2 \, M_R}{M \, \lambda^2 \, F(\beta)}$$

$$\times \sum_{n=1}^{\infty} \left\{ \frac{1}{n \, (n+1)} \frac{\rho_c^{\,n-1}}{\lambda^n} \left[n \, C_{in}(\alpha) + \rho_c \, B_{in}(\alpha) \right] \right.$$

$$\left. -\frac{1}{n} \frac{\lambda^{n+1}}{\rho_c^{\,n+2}} \left[C_{on}(\beta) - C_{on}(\alpha) + \frac{\rho_c}{n+1} \, B_{on}(\alpha) \right] \right\} P_n^1 (\cos \theta) \tag{24}$$

where

$$B_{in}(\alpha) = \frac{\partial}{\partial \rho} C_{in}(\alpha) = - \frac{P_n^1(\cos \alpha)(1 + 3\cos^2 \alpha)^{\frac{1}{2}}}{\lambda \cos \alpha (\sin \alpha)^{2n-3}} \quad ,$$

and

$$B_{on}(\alpha) = \frac{\partial}{\partial \rho} C_{on}(\alpha) = - \frac{(\sin \alpha)^{2n+5} P_n^1(\cos \alpha)(1 + 3\cos^2 \alpha)^{\frac{1}{2}}}{\lambda \cos \alpha} \quad ,$$

and

$$\frac{1}{\rho} \frac{\partial Q}{\partial \theta} = 0 = \frac{1}{\rho} \left(\frac{\cos \theta}{\rho^2} - \frac{2\bar{\gamma} \cos \theta}{\rho \sin^2 \theta} + \frac{2 M_R}{M \lambda^2 F(\beta)} \right.$$

$$\times \sum_{n=1}^{\infty} {}' \frac{1}{n(n+1)} \left\{ \left(\frac{\rho}{\lambda} \right)^n C_{in}(\alpha) + \left(\frac{\lambda}{\rho} \right)^{n+1} [C_{on}(\beta) - C_{on}(\alpha)] \right\}$$

$$\times \left. \left[\frac{n \cos \theta}{\sin \theta} P_n^1(\cos \theta) - \frac{n+1}{\sin \theta} P_{n-1}^1(\cos \theta) \right] \right) \qquad (25)$$

where the subscript c denotes values at the saddle point.

For n odd (which is required for symmetry relative to the equatorial plane) every term of equation 25 has a factor of cos θ to an odd power and this equation is satisfied throughout the equatorial plane. Prescott[23] has found that saddle points occur only at points where the magnetic field is parallel to the symmetry axis. Therefore, saddle points are expected only in the equatorial plane for the particular current distribution assumed. The θ coordinate of all saddle points is assumed to be $\pi/2$. The ρ coordinates of the saddle points are found by eliminating $\bar{\gamma}$ between Equation 21 evaluated at Q = -1 and Equation 24 which results in (at θ = π/2)

$$0 = 1 - \frac{1}{\rho_c^2} + \frac{2\,M_R}{M\,\lambda^2\,F(\beta)} \sum_{n=1}^{\infty} \frac{1}{n(n+1)} \left(\left(\frac{\rho}{\lambda}\right)^n \left[(n+1)\,C_{in}(\alpha) + \rho_c\,B_{in}(\alpha)\right] \right.$$

$$\left. - \left(\frac{\lambda}{\rho}\right)^{n+1} \left\{ n\left[C_{on}(\beta) - C_{on}(\alpha)\right] + \rho_c\,B_{on}(\alpha)\right\}\right) P_n^1(0) \qquad . \qquad (26)$$

In practice, values are assumed for the ring current parameters M_R/M, λ and β. Equation 26 is solved by iteration for self consistent values of ρ_c, the ρ coordinate of the saddle point. The value of $\overline{\gamma}_c$, the $\overline{\gamma}$ for which the saddle point occurs, is obtained from Equation 24 using the same parameters M_R/M, λ and β and the ρ and θ coordinates of the saddle point. $\overline{\gamma}_c$ is given by

$$\overline{\gamma}_c = -\frac{1}{\rho_c} + \frac{M_R}{M\,\lambda\,F(\beta)} \sum_{n=1}^{\infty} \left\{ \frac{1}{n(n+1)} \left(\frac{\rho}{\lambda}\right)^{n+1} \left[n\,C_{in}(\alpha) + \rho_c\,B_{in}(\alpha)\right]\right.$$

$$\left. - \frac{1}{n}\left(\frac{\lambda}{\rho_c}\right)^n \left[C_{on}(\beta) - C_{on}(\alpha) + \frac{\rho_c}{n+1}\,B_{on}(\alpha)\right]\right\} P_n^1(0) \qquad . \qquad (27)$$

For low energy particles the current sheet falls inside the inner forbidden region and there is only one saddle point and it occurs outside the current sheet. For higher energy particles, the Q surface has two saddle points, one between the origin and the current sheet and the other beyond the current sheet.

STÖRMER PLOTS

Störmer plots of allowed and forbidden regions of particle motion for the combination field of the dipole plus the distributed ring current are shown in Figures 3 through 10. The plots were calculated for impact parameters $\overline{\gamma}_c$ such that saddle points occur in the Q surface and pass points occur in the Störmer plots. The regions of forbidden motion are shaded and the allowed regions are unshaded. In the allowed regions $|Q| \leqq 1$ and in the forbidden regions $|Q| > 1$. The Störmer plot for a dipole alone is shown in Figure 3. For a dipole field ($M_R/M = 0$) and $\overline{\gamma} = -1$ there are four regions: an inner forbidden region, $Q > +1$, which is completely shielded from all particles from infinity; an inner allowed region where $-1 \leqq Q \leqq 1$, which is partially shielded from particles from infinity; an outer forbidden region where $Q < -1$ and an outer allowed region where $-1 < Q < 0$, which are both completely unshielded from particles from infinity.

Unlike the Störmer plots for the dipole field which are the same for particles of all energies, the plots for a dipole plus a ring current are strongly dependent on particle energy. This is due primarily to the change in dimensionless ring radius, λ, with the change in the Störmer unit of length. Figure 4 shows the allowed and forbidden regions for the geomagnetic dipole ($\mu M = 1.01788 \times 10^{17}$ weber meters) and a ring current such that a = 6 earth radii, $M_R/M = 0.4$ and $\beta = 30°$ for proton kinetic energy 50 MeV. For this particle energy, the ring current falls within the inner allowed region and the plot is almost the same as for a dipole with the magnetic moment of 1.4 multiplied by the original. The pass point moves from $\rho_c = 1$ to $\rho_c = 1.197$ and the critical impact parameter changes to $\overline{\gamma}_c = -1.1877$. Figures 5, 6 and 7 show the change in the Störmer plots with increasing particle energy while the ring parameters remain the same as in Figure 4. In Figure 5 the proton kinetic energy is 0.1 BeV and the ring current falls just outside the inner forbidden region

19
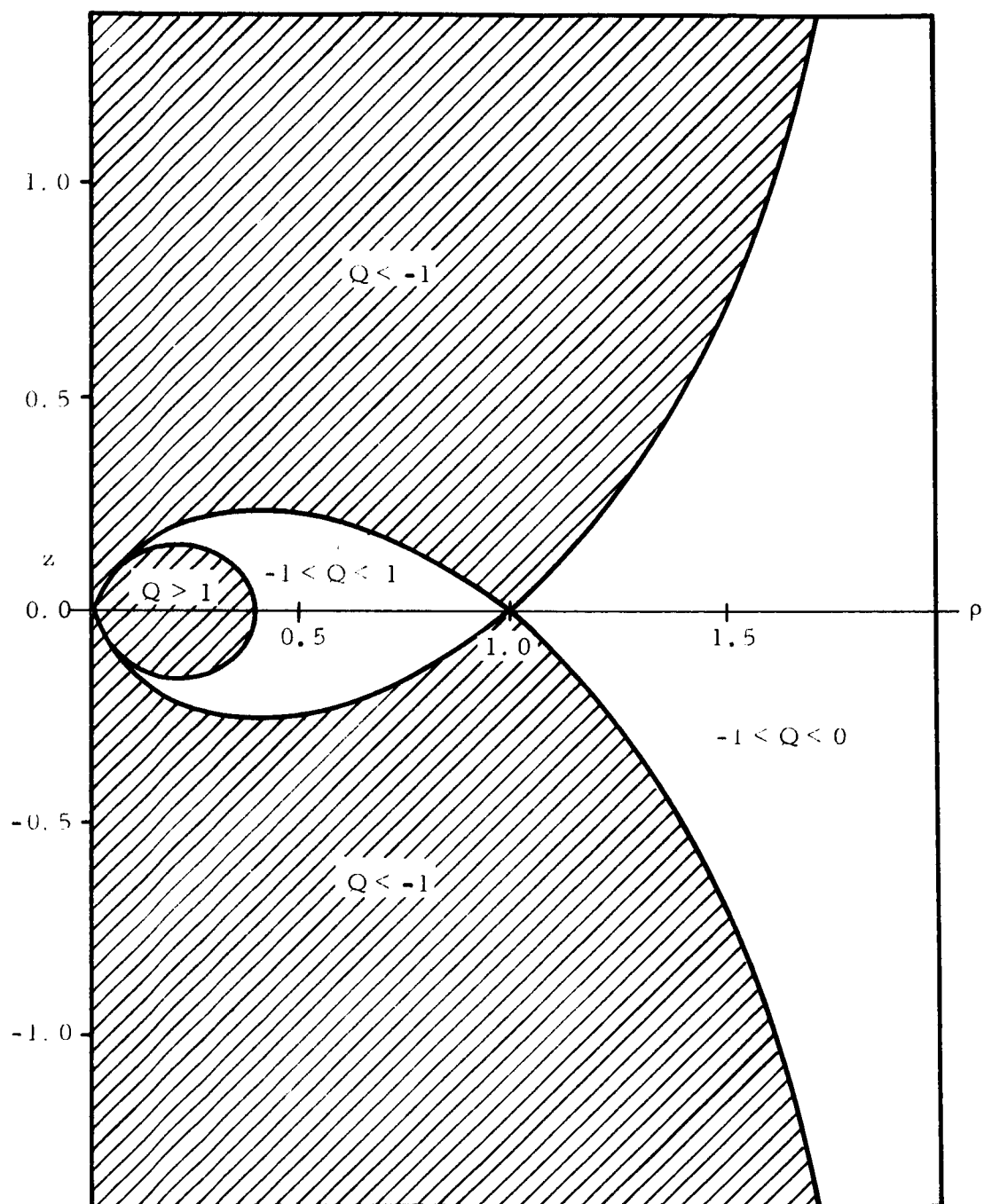
Figure 5. Allowed and Forbidden Regions for a
Dipole, $\overline{\gamma}_c = -1$

Figure 4. Störmer Plot for the Geomagnetic Dipole Plus a
Distributed Ring Current with $M_R/M = 0.4$,
$a = 6$ Earth Radii, $\beta = 30°$ and Protons with 50 MeV
Kinetic Energy, $\overline{\gamma}_c = -1.18766$

Figure 5. Störmer Plot for the Geomagnetic Dipole Plus a
Distributed Ring Current with $M_R/M = 0.4$,
$a = 6$ Earth Radii, $\beta = 30°$ and Protons with
0.1 BeV Kinetic Energy, $\overline{\gamma}_c = -1.18965$

Figure 6. Störmer Plot for the Geomagnetic Dipole Plus a
Distributed Ring Current with M_R/M = 0.4,
a = 6 Earth Radii, β = 30° and Protons with 0.5 BeV
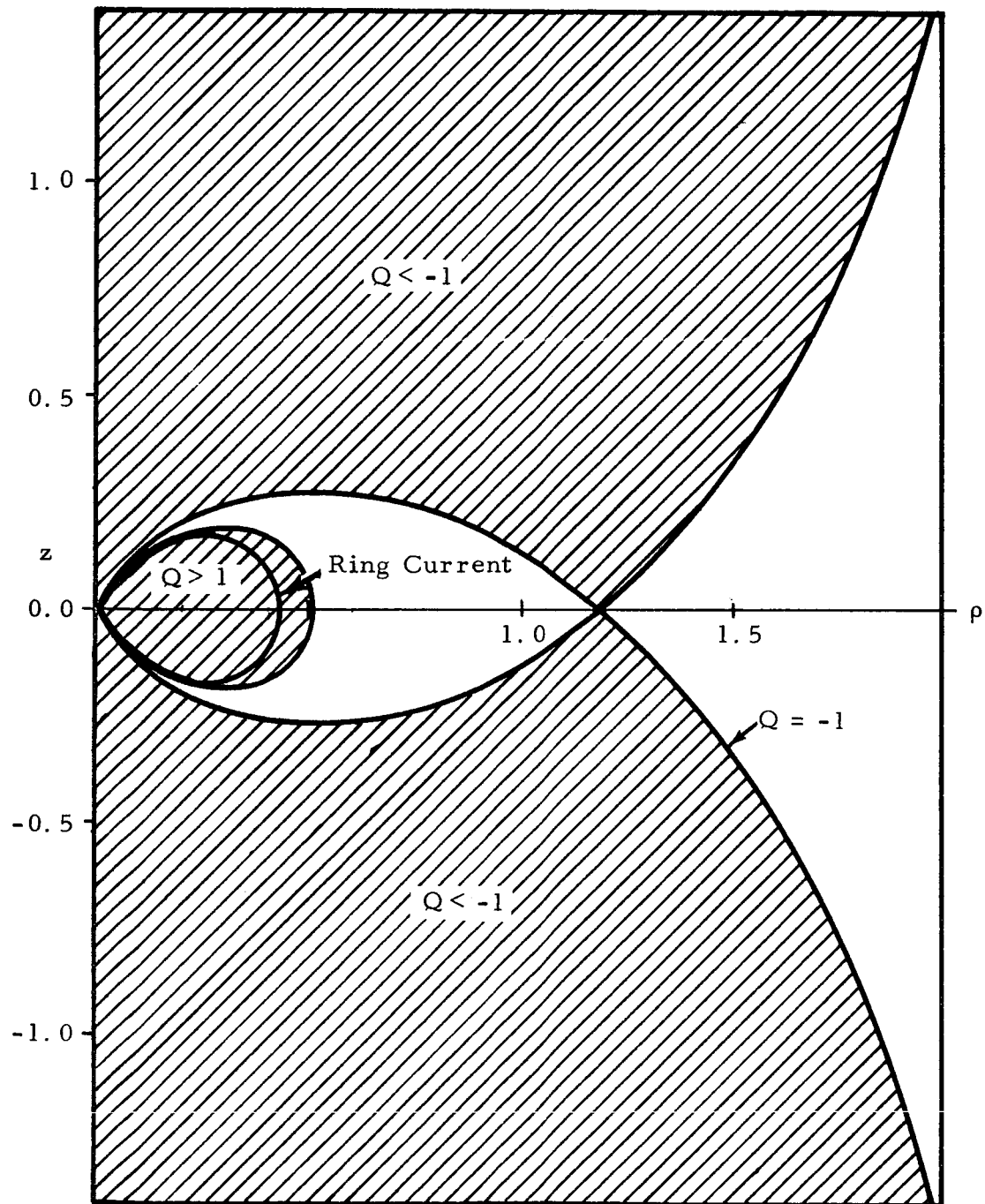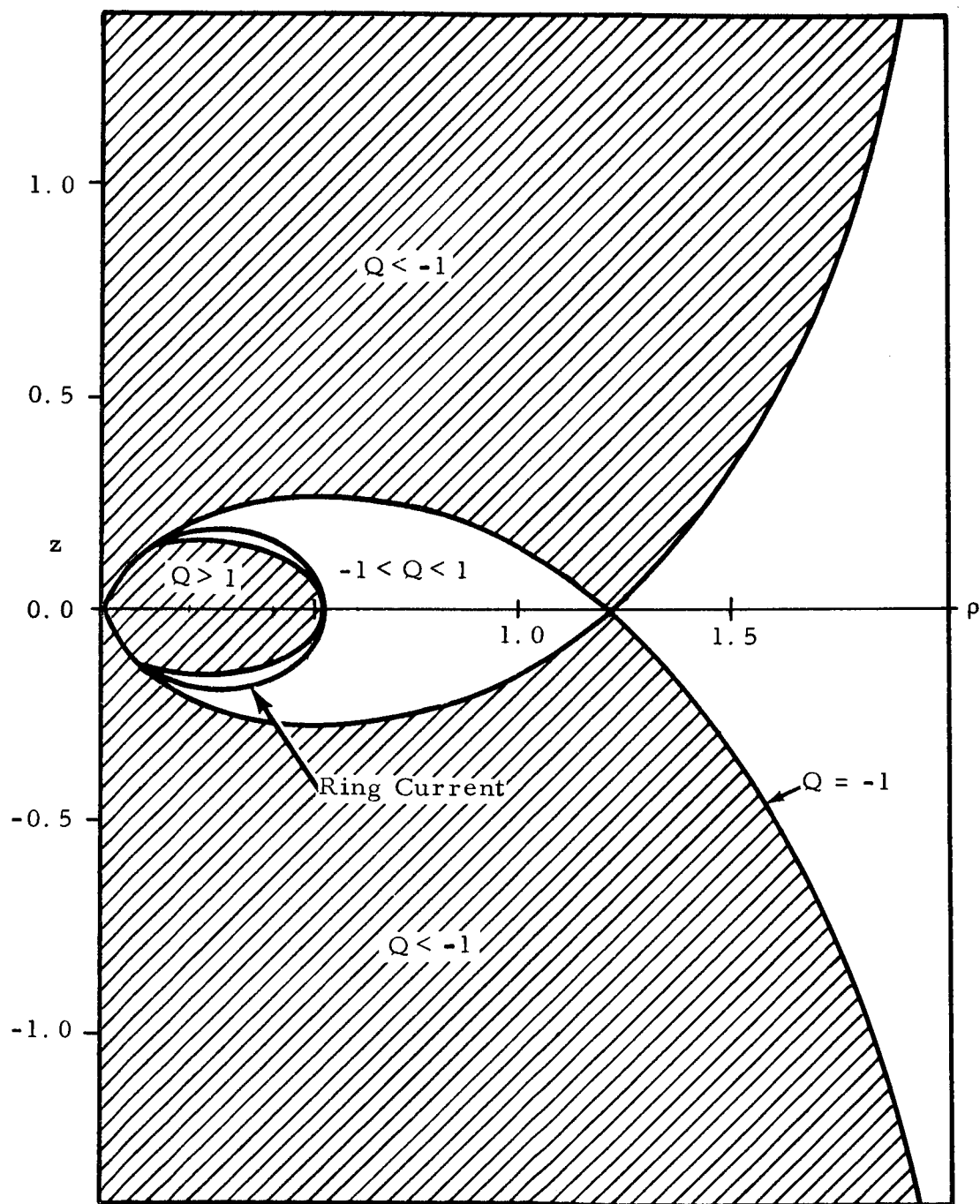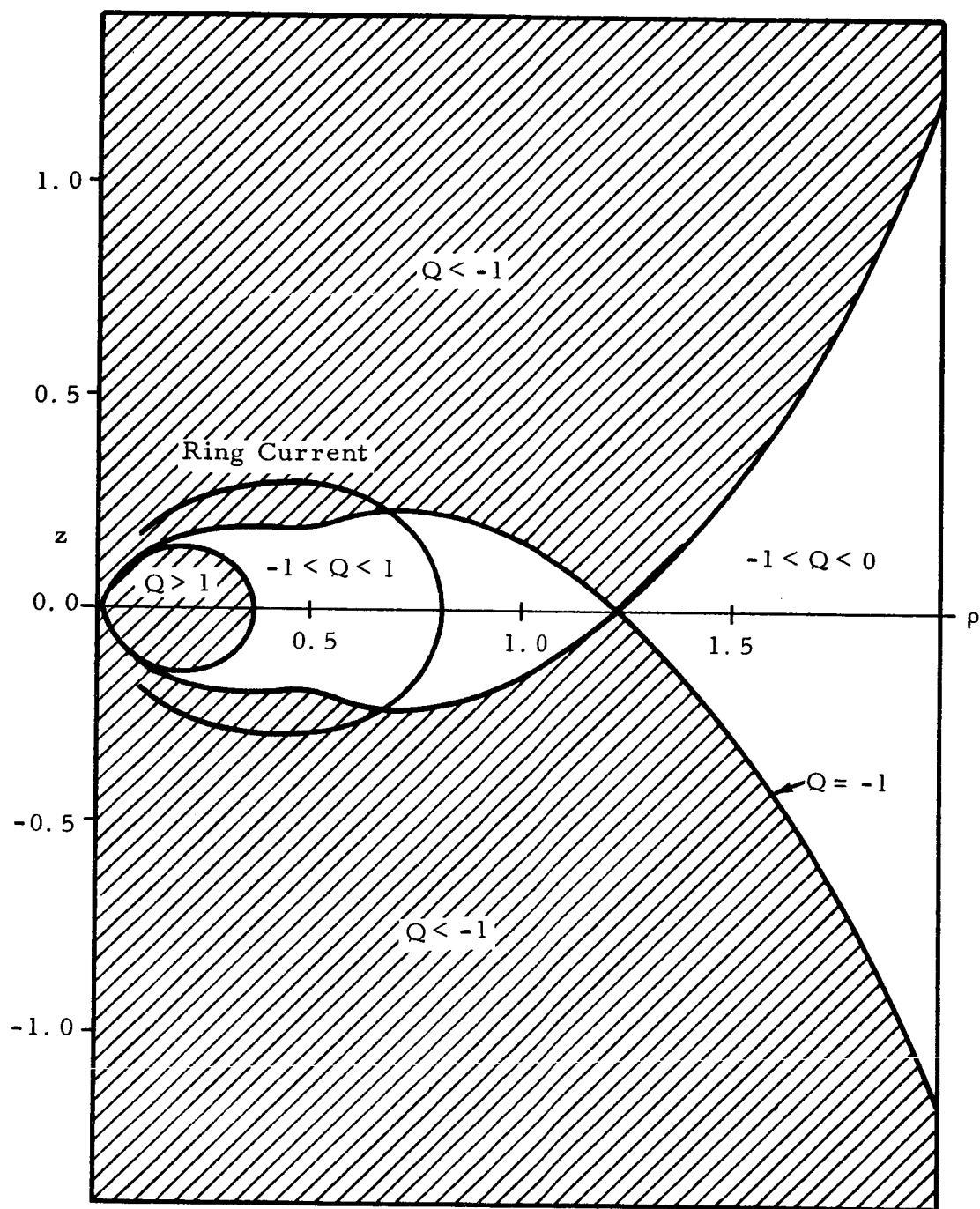Kinetic Energy, $\overline{\gamma}_c$ = -1.19987

23

Figure 7.   Störmer Plot for the Geomagnetic Dipole Plus a
Distributed Ring Current with M_R/M = 0.4,
a = 6 Earth Radii, β = 30° and Protons with
0.5 BeV Kinetic Energy and $\overline{\gamma}_c$ = -1.30895

and the Störmer plot is still essentially that of a dipole with the saddle point occurring in the Q hypersurface at $\rho = 1.203$ and $\overline{\gamma}_c = -1.1898$. The result is an increase in the dimensions of the completely shielded region and the partially shielded region. Figure 6 and 7 show the allowed and forbidden regions for protons with kinetic energy 0.5 BeV for critical impact parameters $\overline{\gamma}_c = -1.19987$ and -1.30895, respectively. These two figures illustrate the occurrence of two saddle points in the Q hypersurface at different impact parameters. The outer pass point (Figure 6) closes for a smaller impact parameter than the inner saddle point (Figure 7). Since particles cannot cross a forbidden region to enter an allowed region, the outer saddle point determines the totally shielded and partially shielded regions. The totally shielded region about the current element which was observed in the case of the filamentary ring current[5, 16, 20, 21] is not observed where the current is distributed over large dimensions. The pass point in Figure 7 is apparently unimportant when considering particles coming from infinity.

Figures 8, 9 and 10 present the allowed and forbidden regions, assuming a ring current with $M_R/M = 0.2222$, radius, $a = 6\ r_e$, $\beta = 30°$ and a sine squared current distribution in the distributed ring. The radius and magnetic moment of this ring current correspond to the V_3 belt of Akasofu and Chapman[10].

As particle energy is increased (from that of Figure 7) the point is reached at which both the inner and the outer saddle points occur for the same impact parameter and for higher energy particles the inner saddle point occurs for smaller $|\overline{\gamma}_c|$. Figures 8 and 9 show the allowed and forbidden regions for protons of kinetic energy 1 BeV and critical impact parameters -1.1175 and -1.12536, respectively. In this case the $\overline{\gamma}_c$ for the inner saddle point determines the totally shielded inner forbidden region and the partially shielded region which extends to the inner pass point. The $\overline{\gamma}_c$ which closes the outer pass point determines the forbidden and allowed regions for $\rho > \rho_{ci}$ where ρ_{ci} is the radial coordinate of the inner saddle point.
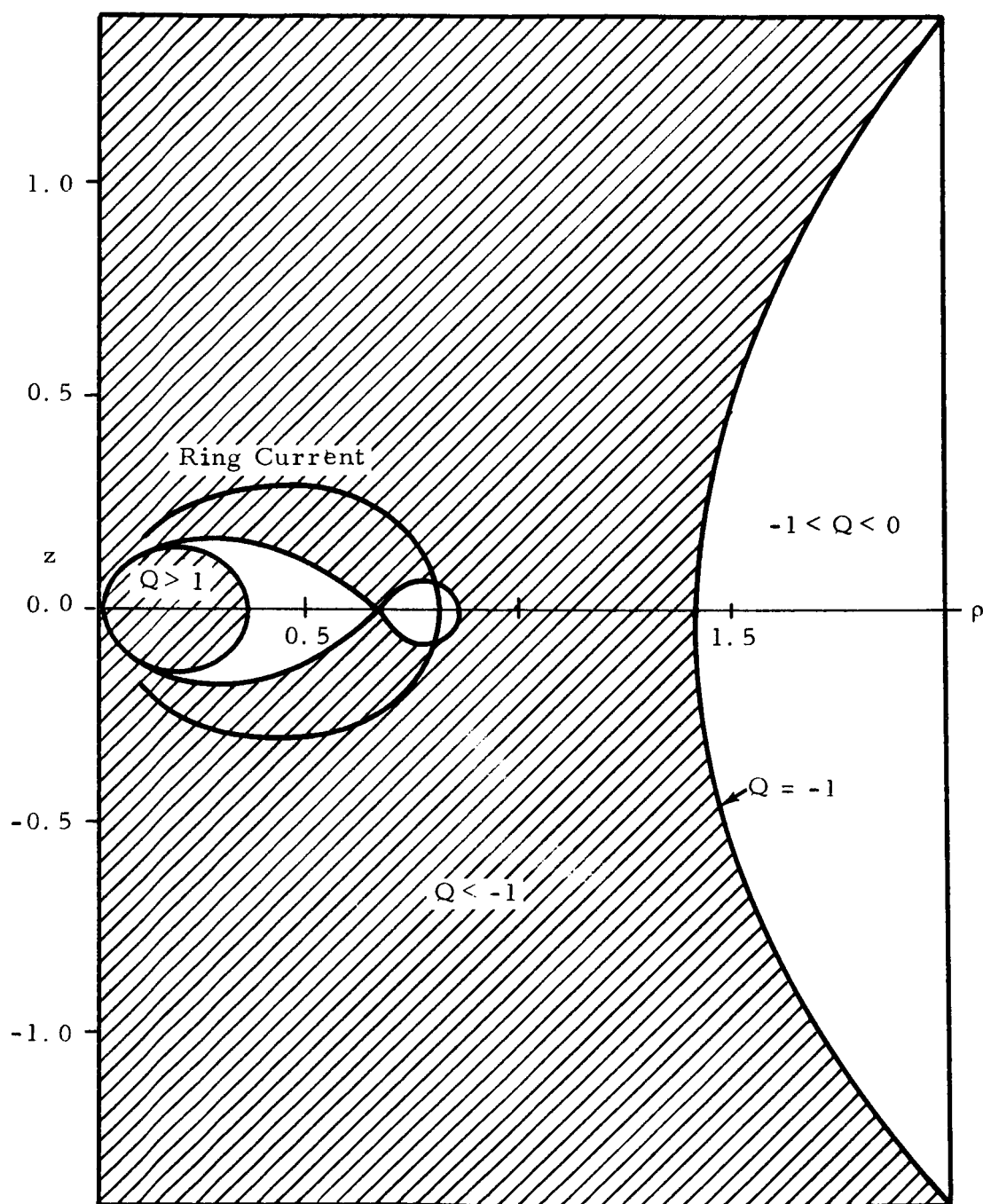
Figure 8. Störmer Plot for the Geomagnetic Dipole Plus a
Distributed Ring Current with M_R/M = 0.2222,
a = 6 Earth Radii, β = 30° and Protons with 1 BeV
Kinetic Energy, $\overline{\gamma}_c$ = -1.11753
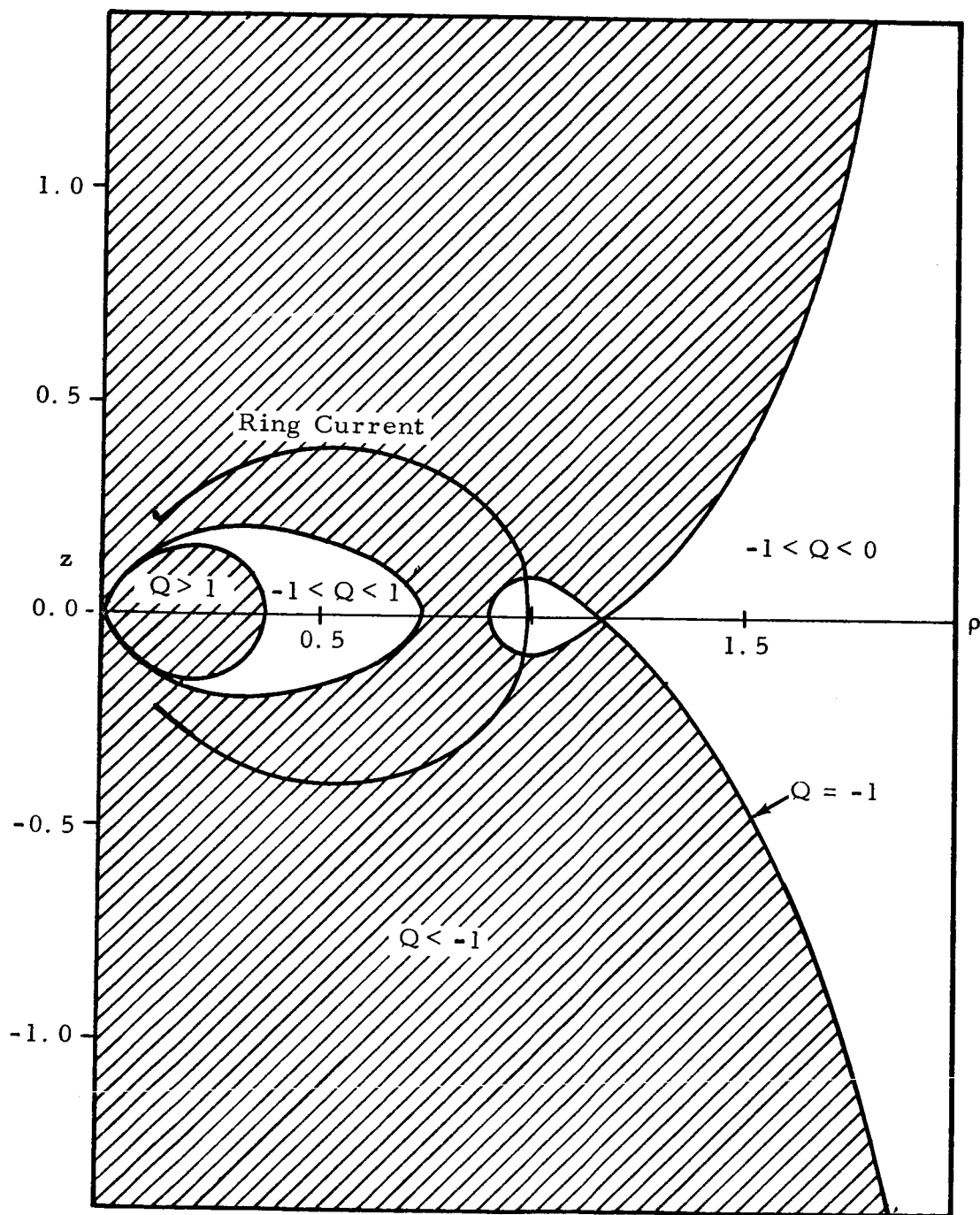
Figure 9. Störmer Plot for the Geomagnetic Dipole Plus a
Distributed Ring Current with $M_R/M = 0.2222$,
$a = 6$ Earth Radii, $\beta = 30°$ and Protons with 1 BeV
Kinetic Energy and $\overline{\gamma}_c = -1.12536$

27

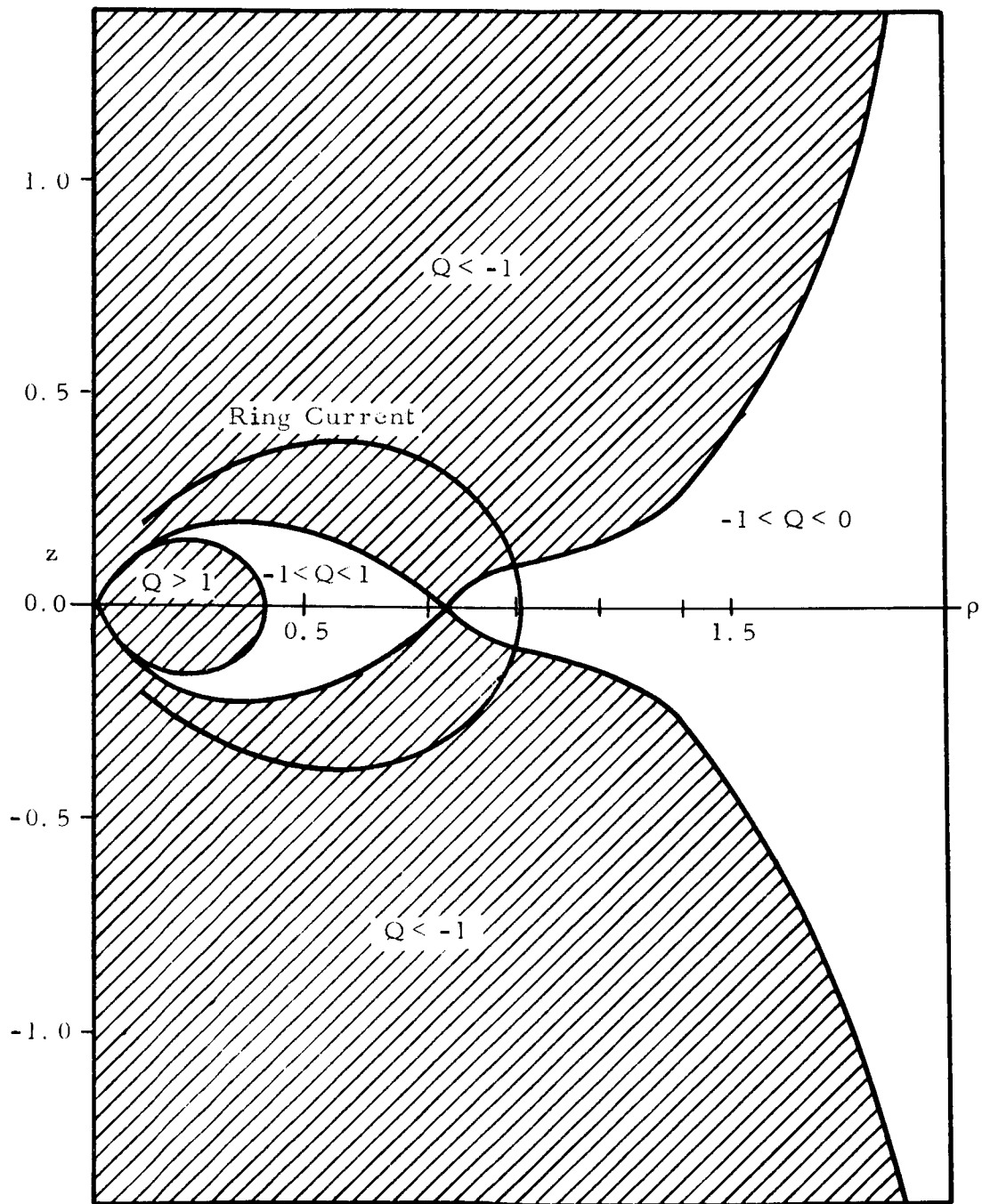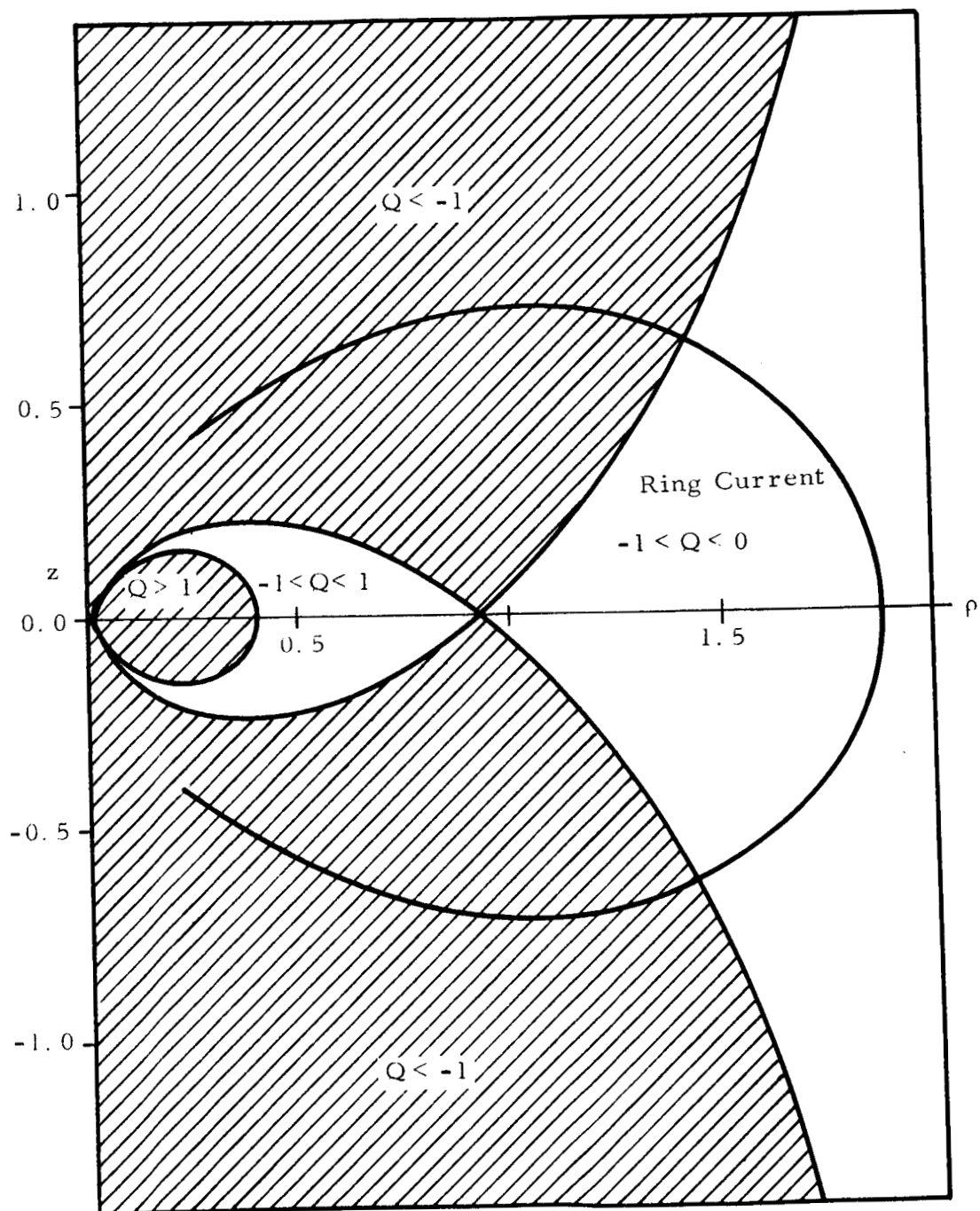Figure 10. Störmer Plot for the Geomagnetic Dipole Plus a Distributed Ring Current with $M_R/M = 0.2222$, $a = 6$ Earth Radii, $\beta = 30°$ and Protons with 5 BeV Kinetic Energy and $\overline{\gamma}_c = -1.0246$

28

For higher proton kinetic energies, the inner saddle point becomes more important. Figure 10 shows the forbidden regions for protons with kinetic energy 5 BeV for the critical impact parameter $\overline{\gamma}_c = -1.04288$ which just closes the inner region. The Störmer plot again looks very similar to the dipole plot. In this case, however, the ring current reduces the volumes of the totally shielded and partially shielded regions instead of increasing them as in the case of low energy particles. The volume of the shielded and partially shielded regions decreases with increasing ring current.

UNBOUND PARTICLE FLUX CALCULATION

The ratio of the untrapped proton flux at points inside the magneto-
sphere to an isotropic and spatially uniform flux at infinite distance can be
calculated using the Störmer transformation and Liouville's theorem. The
technique is discussed in the literature[22, 24, 25, 26] and will only be sum-
marized here.

Liouville's theorem states that the distribution function, $f(\vec{r}, \vec{P})$,
in six-dimensional phase space, $(\vec{r}, \vec{P})$, is a constant of the motion, where
the components of $\vec{P}$ are the conjugate momenta of the components of $\vec{r}$ of
the Hamiltonian equations of motion and $\vec{P} = \vec{p} + q\vec{A}$. Swann[24] has shown
that the distribution function $f(\vec{r}, \vec{p})$ is also a constant of the motion in the
quasi-phase space $(r, \vec{p})$. If particle energy and speed remain constant,
the distribution function is constant along a particle trajectory connecting
two points in real space.

For monoenergetic particles the flux at a position $\vec{r}$ is defined by

$$\Phi(\vec{r}, E) = \int_{\Omega} v_E \, f(\vec{r}, \vec{v}_E) \, d\Omega \qquad (28)$$

where $\vec{v}_E$ is a velocity corresponding to energy E and the integration is
over the solid angle containing all directions from which particles are
allowed to arrive. The Störmer allowed cone contains all the allowed
directions and it has been shown[27] that, neglecting the shadow effect, the
flux is uniform over the allowed cone and the flux at $\vec{r}$ is given by

$$\Phi(\vec{r}, E) = v_E \, f(\vec{r}, v_E) \int_{\Omega} d\Omega \qquad . \qquad (29)$$

The half angle of the allowed cone is $\cos^{-1} Q$ where Q is given by
Equation 21. The differential element of solid angle is given by

$$d\Omega = \sin \omega \, d\omega \, d\delta$$

where δ is the azimuthal angle of the right circular Störmer cone. Therefore,

$$\int d\Omega = -\int_0^{2\pi} \int_{Q_1}^{Q_2} dQ\, d\delta = -2\pi\,(Q_2 - Q_1)$$

$$= 2\pi\,(Q_1 - Q_2) \qquad . \tag{30}$$

The flux at $\vec{r}$ is given by

$$\Phi(\vec{r}, E) = 2\pi\, v_E\, f(\vec{r}, v_E)\,(Q_1 - Q_2) \qquad . \tag{31}$$

The assumption that v, p and E are constant along with Liouville's theorem lead to

$$v\, f(\vec{r}, v) = v\, f(\vec{r}_\infty, v) \qquad , \tag{32}$$

where $\vec{r}_\infty$ is a point at infinite distance. The flux of particles of energy E at infinity is given by

$$\Phi(r_\infty, E) = \int_{\Omega_\infty} v_E\, f(\vec{r}_\infty, \vec{v}_E)\, d\Omega = 4\pi\, v_E\, f(\vec{r}_\infty, \vec{v}_E) \tag{33}$$

since the flux at infinity is assumed to be isotropic and spatially uniform.

The ratio of flux at $\vec{r}$ to the flux at infinity is given by

$$\frac{\Phi(\vec{r}, E)}{\Phi(\vec{r}_\infty, E)} = \frac{1}{2}\,[Q_1(\vec{r}, E) - Q_2(\vec{r}, E)]$$

$$= \frac{1}{2}\,[Q_1(\rho) - Q_2(\rho)] \qquad . \tag{34}$$

The Störmer cone is completely closed at $Q = +1$ which is the lower limit, Q_1 of the integral just evaluated, and the cone is fully open at $Q = -1$. The upper limit Q_2 is the value of $Q(\bar{\gamma}_c)$ calculated using Equation 21.

For dipole fields, Prescott[22] has shown that the ratio of the unbound particle flux at $\vec{r}$ to an isotropic flux at $r = \infty$ is given by

$$\frac{\Phi(\vec{r})}{\Phi(\vec{r}_\infty)} = 0 \text{ if } Q_C \geqq 1 \qquad \begin{array}{l}\text{Inner forbidden region} \\ \text{(completely shielded)}\end{array} \qquad (35)$$

$$\frac{\Phi(\vec{r})}{\Phi(\vec{r}_\infty)} = \frac{1}{2}(1 - Q_C) \text{ if } -1.0 \leqq Q_C < 1.0 \text{ and } \frac{\partial Q_C}{\partial \rho} < 0$$

$$\begin{array}{l}\text{Inner allowed region} \\ \text{(partially shielded)}\end{array} \qquad (36)$$

$$\frac{\Phi(\vec{r})}{\Phi(\vec{r}_\infty)} = 1 \text{ if } Q_C < -1 \qquad \begin{array}{l}\text{Outer forbidden region or if} \\ -1 < Q_C < 0 \text{ and } \partial Q_C / \partial \rho > 0 \\ \text{Outer allowed region} \\ \text{(completely unshielded region)}\end{array} \qquad (37)$$

where $Q_C = Q(\overline{\gamma}_C)$.

Similar equations were found to apply in the case of the ring current. The only modification required to obtain the flux ratios for the filamentary ring is the replacment of $\partial Q_C / \partial \rho$ by $\partial Q_C / \partial \tilde{\rho}$ where $\tilde{\rho}$ is measured from the ring rather than its center.

Examination of the allowed and forbidden regions of Störmer space for the dipole plus a ring current (filamentary or distributed) leads to the following results. In general two saddle points may be found in the Q hypersurface, and these saddle points occur for different values of critical impact parameter $\overline{\gamma}_{ci}$ and $\overline{\gamma}_{co}$ for the inner and outer saddle points, respectively. If $|\overline{\gamma}_{co}| < |\overline{\gamma}_{ci}|$, the outer pass point closes first as impact parameter is becoming more negative and the inner allowed regions for the dipole and for the ring current are connected. Figures 4 through 6 are examples of this situation and the flux ratios are calculated using the following rules:

33

For $|\overline{\gamma}_{co}| < |\overline{\gamma}_{ci}|$,

$$Q_c = Q_c \, (\overline{\gamma}_{co})$$

$$\frac{\Phi(\vec{r})}{\Phi(\vec{r}_\infty)} = 0 \text{ if } Q_c \gtreqless + 1$$

$$\frac{\Phi(\vec{r})}{\Phi(\vec{r}_\infty)} = \frac{1}{2} \, (1 - Q_c) \text{ if } - 1.0 \le Q_c < 1.0 \text{ and } \rho < \rho_{co}$$

$$\frac{\Phi(\vec{r})}{\Phi(\vec{r}_\infty)} = 1 \text{ if } Q_c < - 1 \text{ or if } - 1 < Q < 0 \text{ and } \rho > \rho_{co} \qquad (38)$$

where ρ_{co} is the ρ coordinate of the outer saddle point. These equations apply to the lower energy part of the spectrum but the energy at which they cease to apply depends on the ring parameters.

For the higher energy particles $|\overline{\gamma}_{ci}| < |\overline{\gamma}_{co}|$ and the inner pass point closes first as $\overline{\gamma}$ is becoming more negative. In these cases the inner allowed region for the dipole and the allowed region for the ring current are separate and the rules for calculating flux ratios for the dipole may be applied out to $\rho = \rho_{ci}$ and the rules for the ring current may be applied for $\rho > \rho_{ci}$ where ρ_{ci} is the ρ coordinate of the inner saddle point. Equivalent rules may be stated as follows for $|\overline{\gamma}_{ci}| < |\overline{\gamma}_{co}|$:

$$\frac{\Phi(\vec{r})}{\Phi(\vec{r}_\infty)} = 0 \text{ if } Q \, (\overline{\gamma}_{ci}) \ge 1 \text{ and } \rho < \rho_{ci} \text{ or if}$$
$$Q \, (\overline{\gamma}_{co}) \ge 1 \text{ and } \rho > \rho_{ci}$$

$$\frac{\Phi(\vec{r})}{\Phi(\vec{r}_\infty)} = \frac{1}{2} \, [1 - Q \, (\overline{\gamma}_{ci})] \quad \text{if} - 1 \le Q \, (\overline{\gamma}_{ci}) < 1 \text{ and } \rho < \rho_{ci}$$

$$\frac{\Phi(\vec{r})}{\Phi(\vec{r}_\infty)} = \frac{1}{2} \, [1 - Q \, (\overline{\gamma}_{co})] \quad \text{if} - 1 \le Q \, (\overline{\gamma}_{co}) < 1$$
$$\text{and } \rho_{ci} < \rho < \rho_{co}$$

34

$$\frac{\Phi(\vec{r})}{\Phi(\vec{r}_\infty)} = 1 \text{ if } Q\,(\overline{\gamma}_{ci}) < -1 \text{ and } \rho < \rho_{ci}$$

$$\text{or if } Q\,(\overline{\gamma}_{co}) < -1 \text{ and } \rho > \rho_{ci}$$

$$\text{or if } -1 < Q\,(\overline{\gamma}_{co}) < 0 \text{ and } \rho > \rho_{co} \quad . \tag{39}$$

The ratios of particle flux at $\vec{r}$ to an isotropic flux at infinity were calculated for the geomagnetic dipole plus a filamentary ring and for the geomagnetic dipole plus distributed ring currents using Equations 38 and 39. Calculations were made for a series of proton kinetic energies from 10 MeV to 10 BeV. Flux ratios were also calculated for the geomagnetic dipole field (using Equations 35 through 37) for comparison with the flux ratios for the combination fields. The results of the flux ratio calculations are presented in Figures 11 through 18.

Figures 11 through 14 give flux ratios in the equatorial plane. (Figure 12 is for $\theta = 89.5°$ instead of $90°$ to avoid the singular point in Q at $\left(\lambda, \frac{\pi}{2}\right)$ for the dipole plus a filamentary ring current.) The general influence of the ring current is a reduction of unbound particle flux in the equatorial plane for radial distances greater than or in the vicinity of the ring current. The flux ratios all go to zero at $\left(\lambda, \frac{\pi}{2}\right)$ for the dipole and filamentary ring and the reduction is quite pronounced for $\rho \sim \lambda$ and $\theta = 89.5°$ for this model. The reduction of the ratios in the vicinity of $\rho = \lambda$ for the distributed ring current is much less pronounced in the equatorial plane. For radial distances $\sim 7\text{-}10$ earth radii, the filamentary ring and the distributed ring current produce approximately equal reductions in particle flux provided they have the same magnetic moment. The dipole model predicts that 10 MeV particles will penetrate the magnetosphere to about 8.6 earth radii from the dipole, whereas the combination field models predict total shielding from 10 MeV protons out to about 10 earth radii. Unbound particle flux reductions by a ring current are predicted for all particles not sufficiently energetic to penetrate the ring current. The opposite effect is predicted for particles with sufficient energy to penetrate the inner field. The ring current field subtracts from the dipole
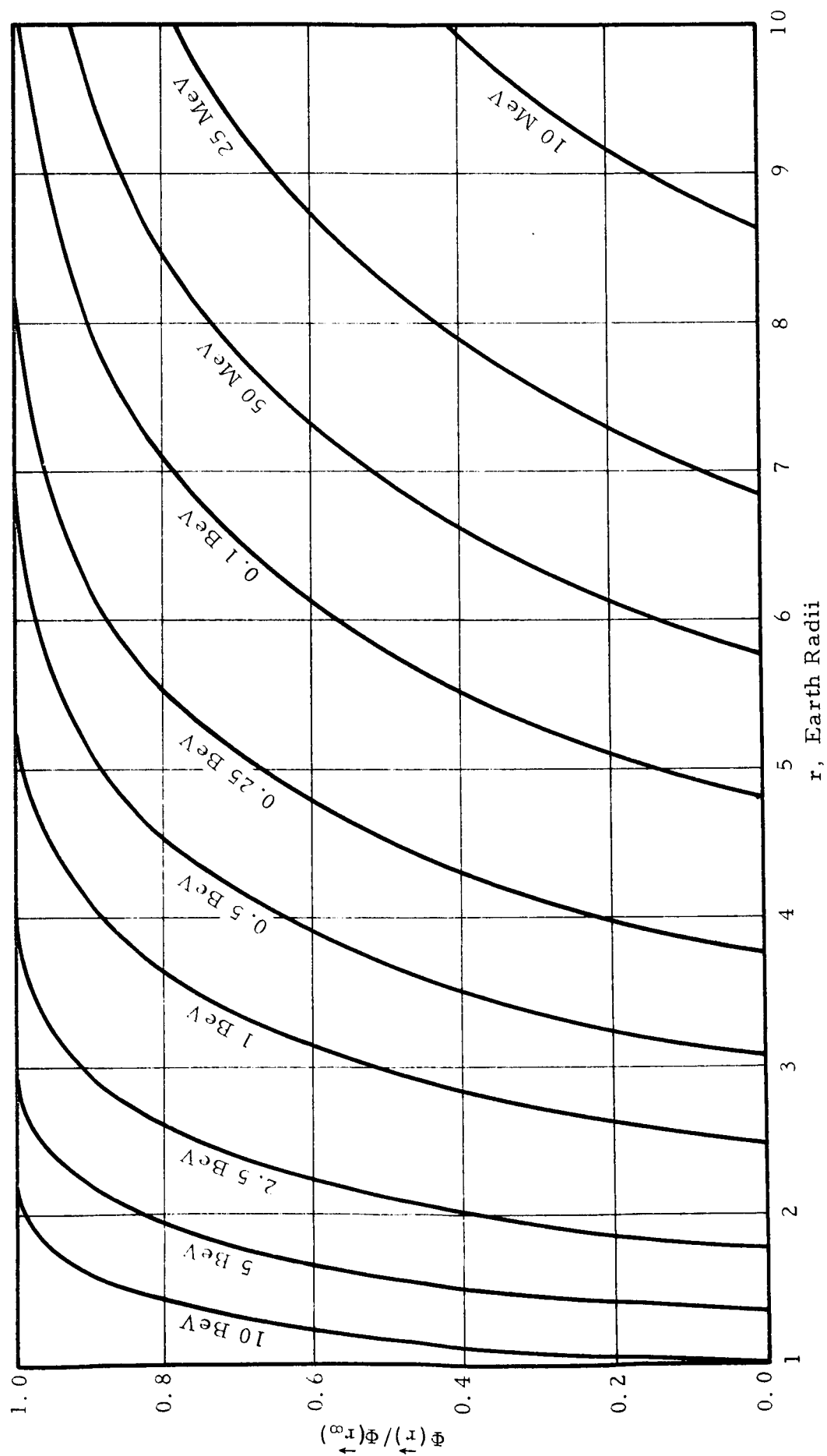
35

Figure 11. Ratio of Proton Flux at r to Flux at Infinity for Geomagnetic Dipole Field, $\mu M = 1.01788 \times 10^{17}$ Wb-m, $\theta = 90°$
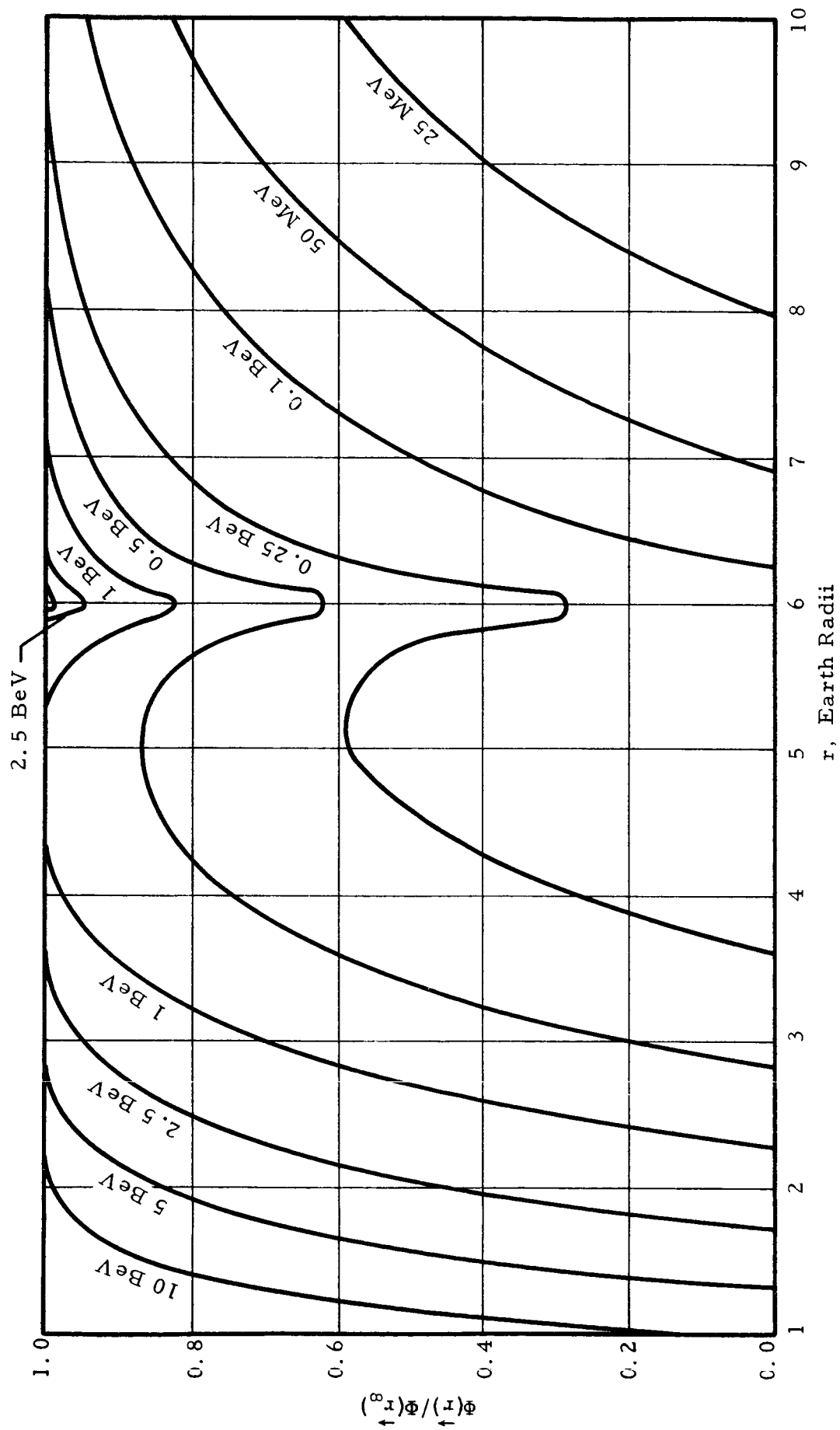
36

Figure 12. Ratio of Proton Flux at $\vec{r}$ to Flux at Infinity for Dipole Plus
Filamentary Ring Current, $M_R/M = 0.2222$, a = 6 Earth Radii
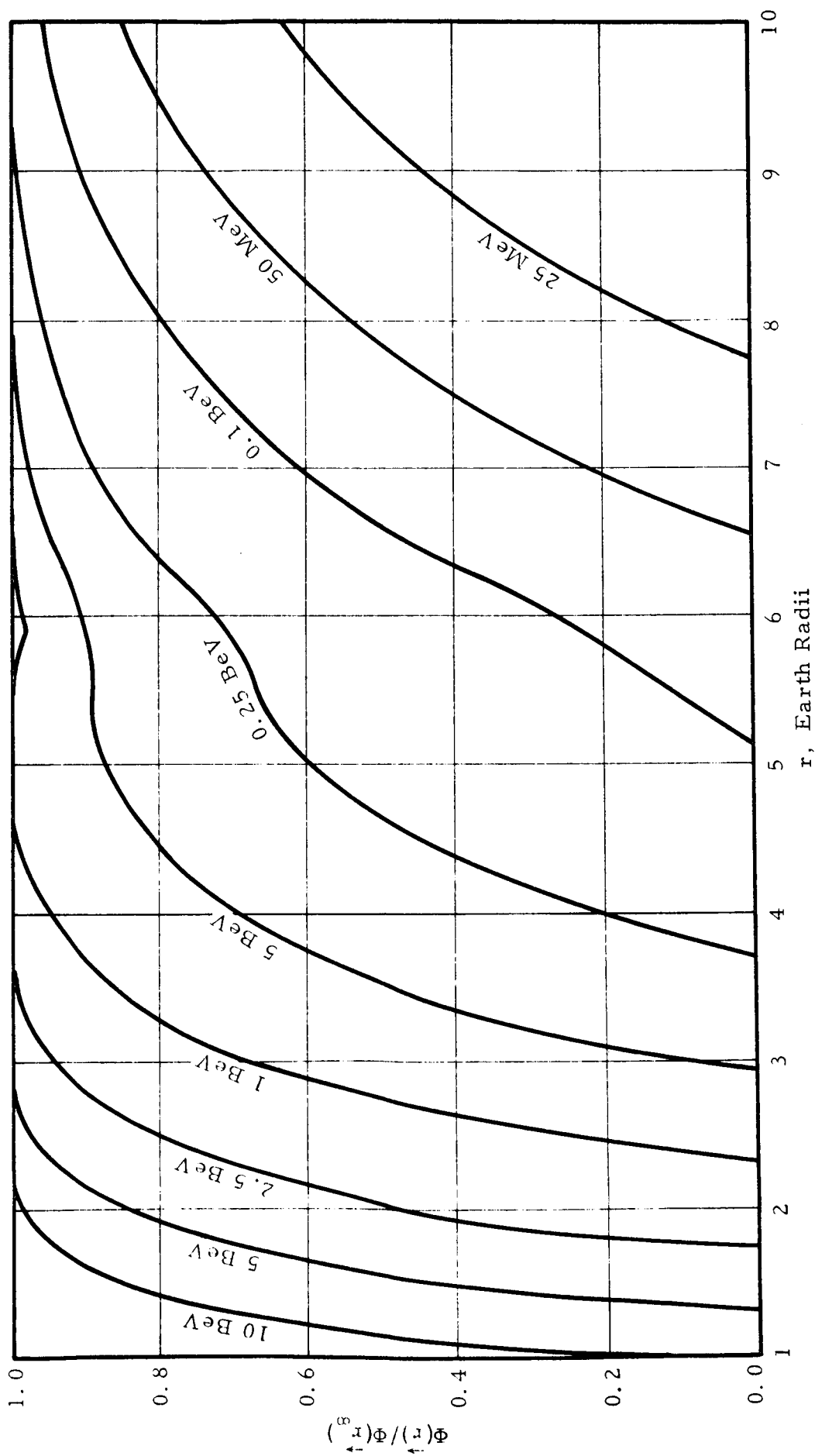$\theta = 89.5°$

37

Figure 13. Ratio of Proton Flux at r to Flux at Infinity for Dipole Plus Distributed Ring Current, $M_R/M = 0.2222$, $a = 6$ Earth Radii, $\beta = 30°$, $\theta = 90°$
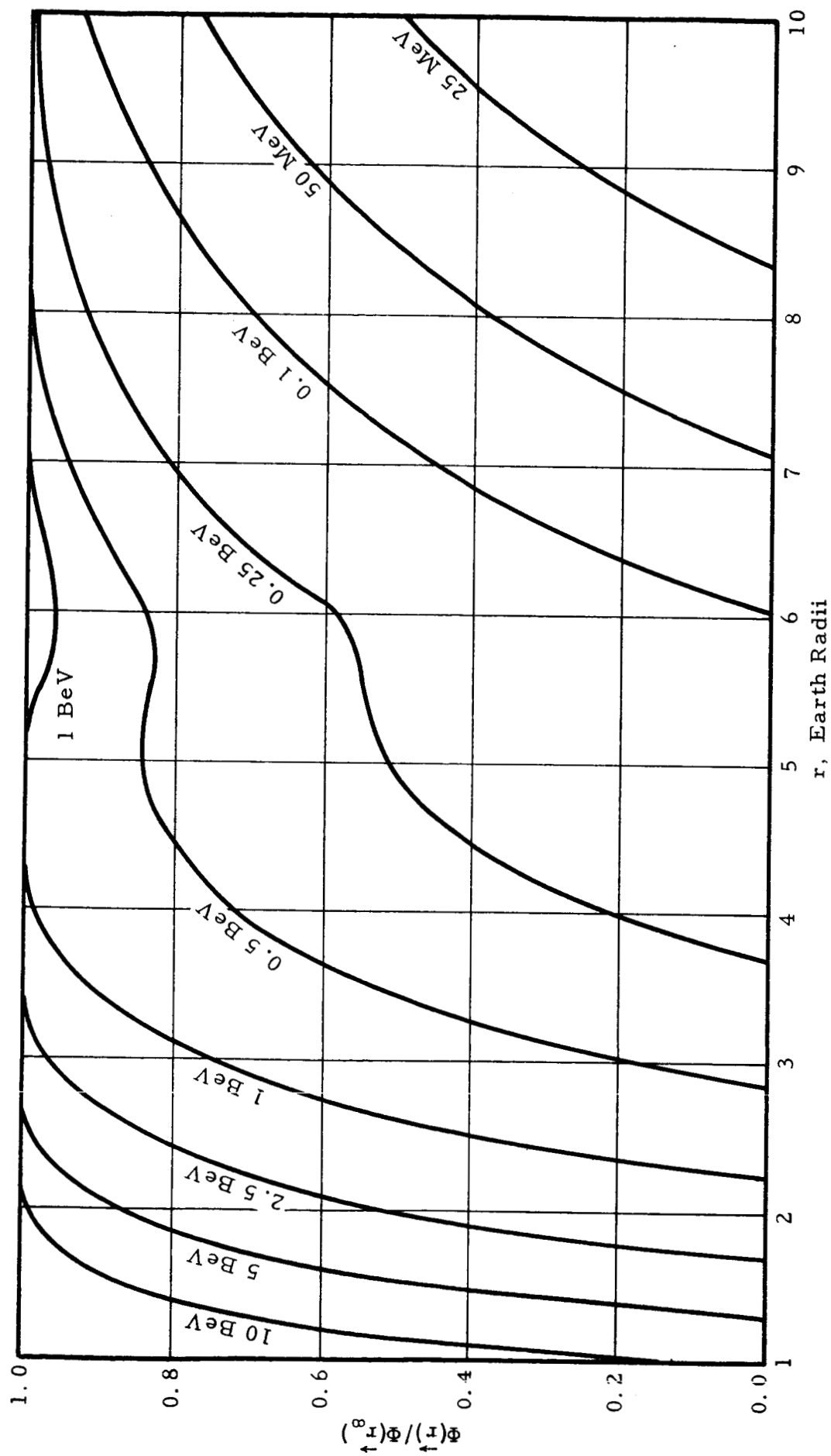
38

Figure 14. Ratio of Proton Flux at $\vec{r}$ to Flux at Infinity for Dipole Plus Distributed Ring Current, $M_R/M = 0.40$, $a = 6$ Earth Radii, $\beta = 30°$, $\theta = 90°$

field for r < a and the effectiveness of the shielding provided by the dipole field is therefore reduced. The effect is manifested at the Earth's surface in the reduction of the cutoff rigidity for cosmic rays[18, 19, 20]. The increase in unbound particle flux about one earth radius from the dipole which is due to the ring current is rather small. For example, the flux ratio for 10 BeV protons at r = 1 is increased from about 0.045 to about 0.135 with the addition of a ring current with $M_R/M \approx 0.4$ at a = 6 r_e. A visual estimate of the average increase in flux ratios due to the ring current of Figure 14 compared to Figure 11 is about 6 per cent over the radial interval $1 r_e < r < 4 r_e$.

Figures 15 through 18 present the results of flux ratio calculations at θ = 80° for the different field configurations being considered. Again the ring current is found to slightly increase the flux ratios near the dipole and decrease the flux ratio in the vicinity of r = a and for r > a. The distributed ring current model leads to preditions of smaller flux ratios in the vicinity r = a than the filamentary ring current model for rings with the same magnetic moment. A comparison of Figures 17 and 18 shows that flux ratios depend strongly on the magnetic moment of the ring current, especially in the vicinity of the ring current and beyond.

Since these flux ratios were calculated using an axisymmetric field model, their values are not valid near the magnetopause. Also the effect of the solid earth which would reduce the particle flux near the Earth was not considered. The particle flux estimates are expected to be too high near the Earth.

Flux ratios at higher magnetic colatitude (θ ≈ 40°) for filamentary and distributed ring currents plus a dipole show that a distributed ring current is less effective than a filamentary ring current of the same magnetic moment in the reduction of cutoff rigidity. Estimates of ring currents required to achieve a certain reduction in cutoff rigidity near the Earth's surface are too low if a filamentary ring current model is used when the actual current is distributed over large volumes.
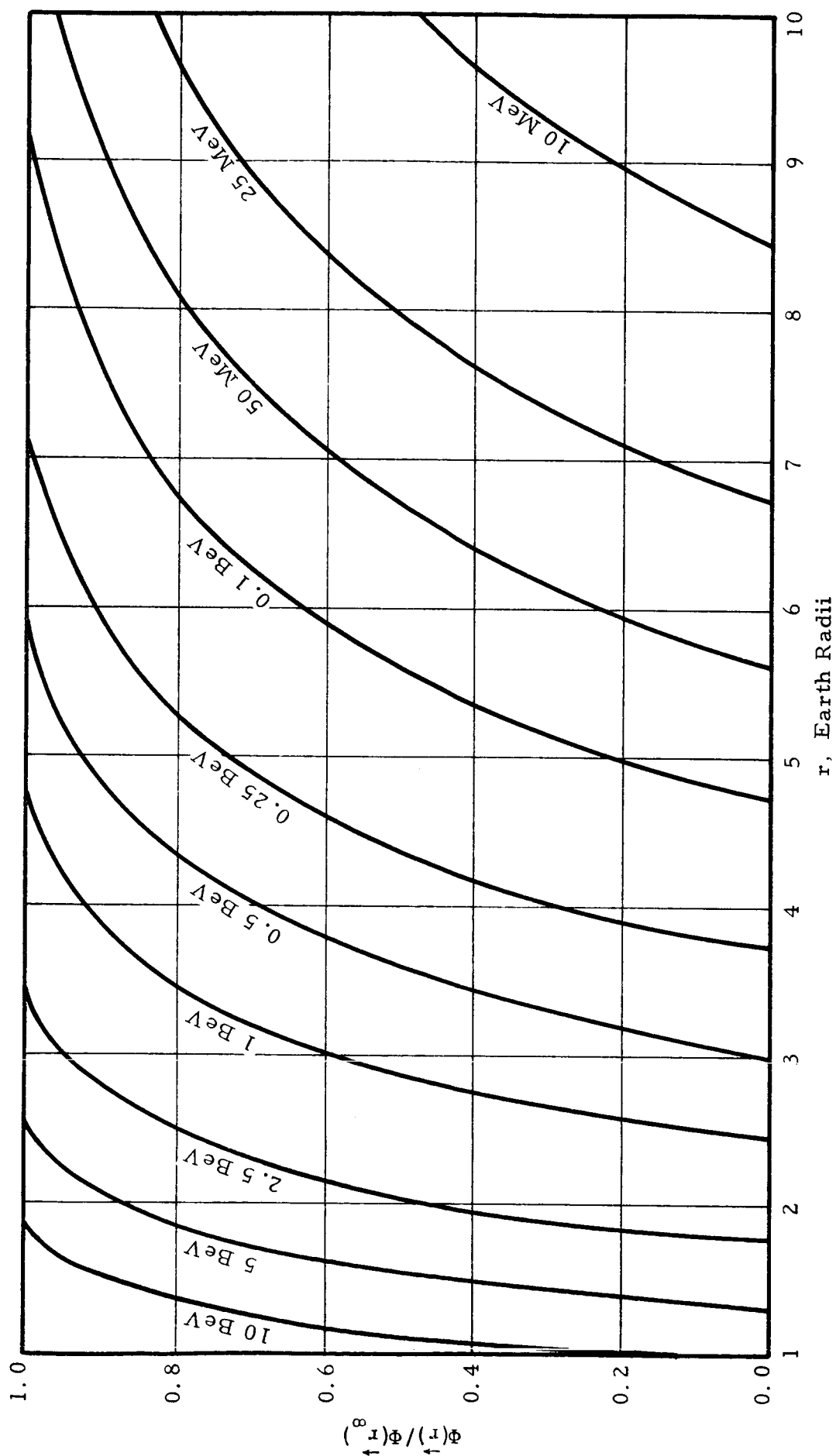
Figure 15. Ratio of Proton Flux at $\vec{r}$ to Flux at Infinity for Geomagnetic Dipole Field, $\mu M = 1.01788 \times 10^{17}$ Wb-m, $\theta = 80°$

41

Figure 16. Ratio of Proton Flux at $\vec{r}$ to Flux at Infinity for Dipole Plus Filamentary Ring Current, $M_R/M = 0.2222$, $a = 6$ Earth Radii, $\theta = 80°$

42

Figure 17. Ratio of Proton Flux at r⃗ to Flux at Infinity for Dipole Plus Distributed Ring Current, $M_R/M = 0.2222$, $a = 6$ Earth Radii, $\beta = 30°$, $\theta = 80°$

43

Figure 18. Ratio of Proton Flux at $\vec{r}$ to Flux at Infinity for Dipole Plus Distributed Ring Current $M_R/M = 0.40$, $a = 6$ Earth Radii, $\beta = 30°$, $\theta = 80°$
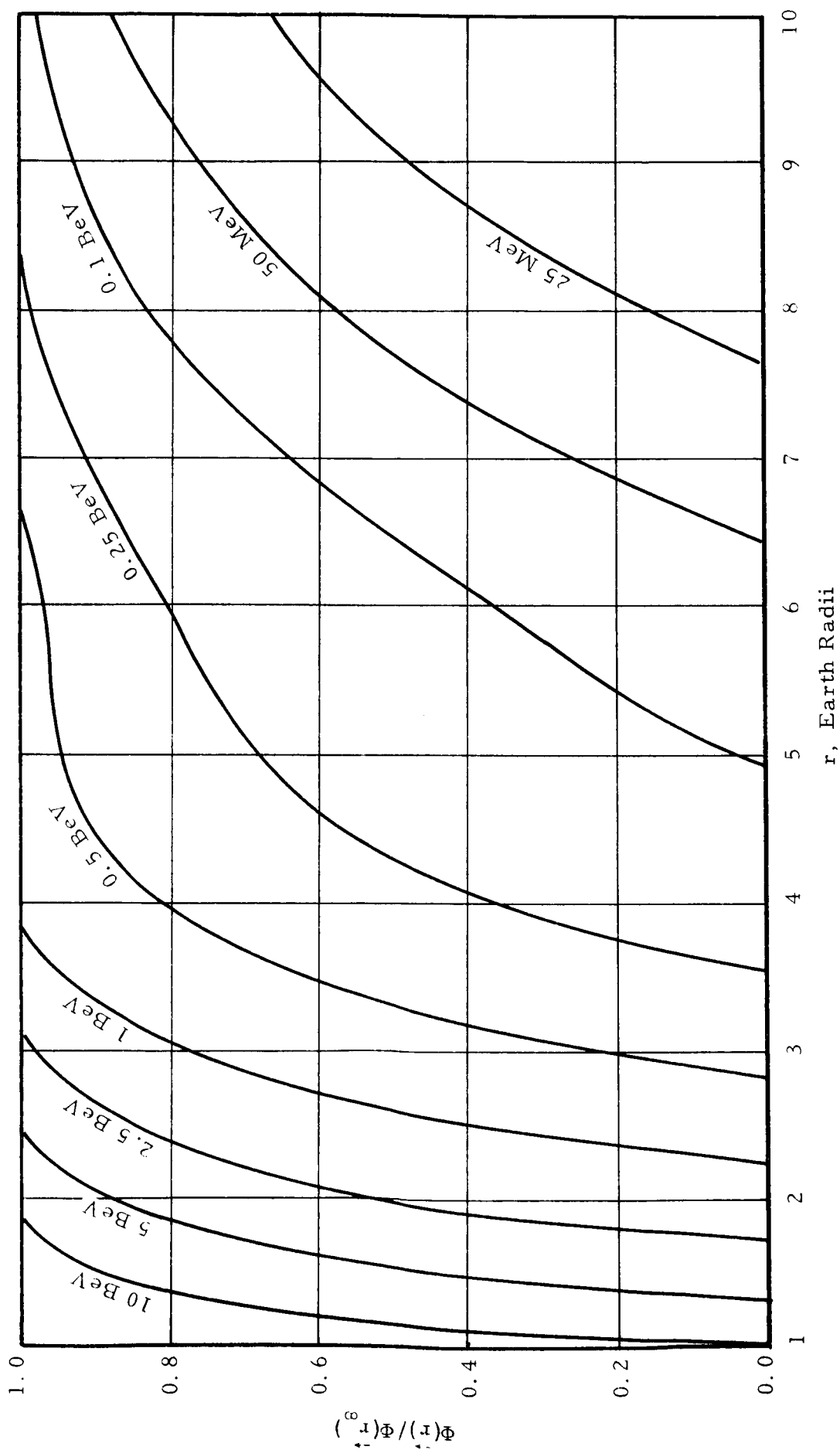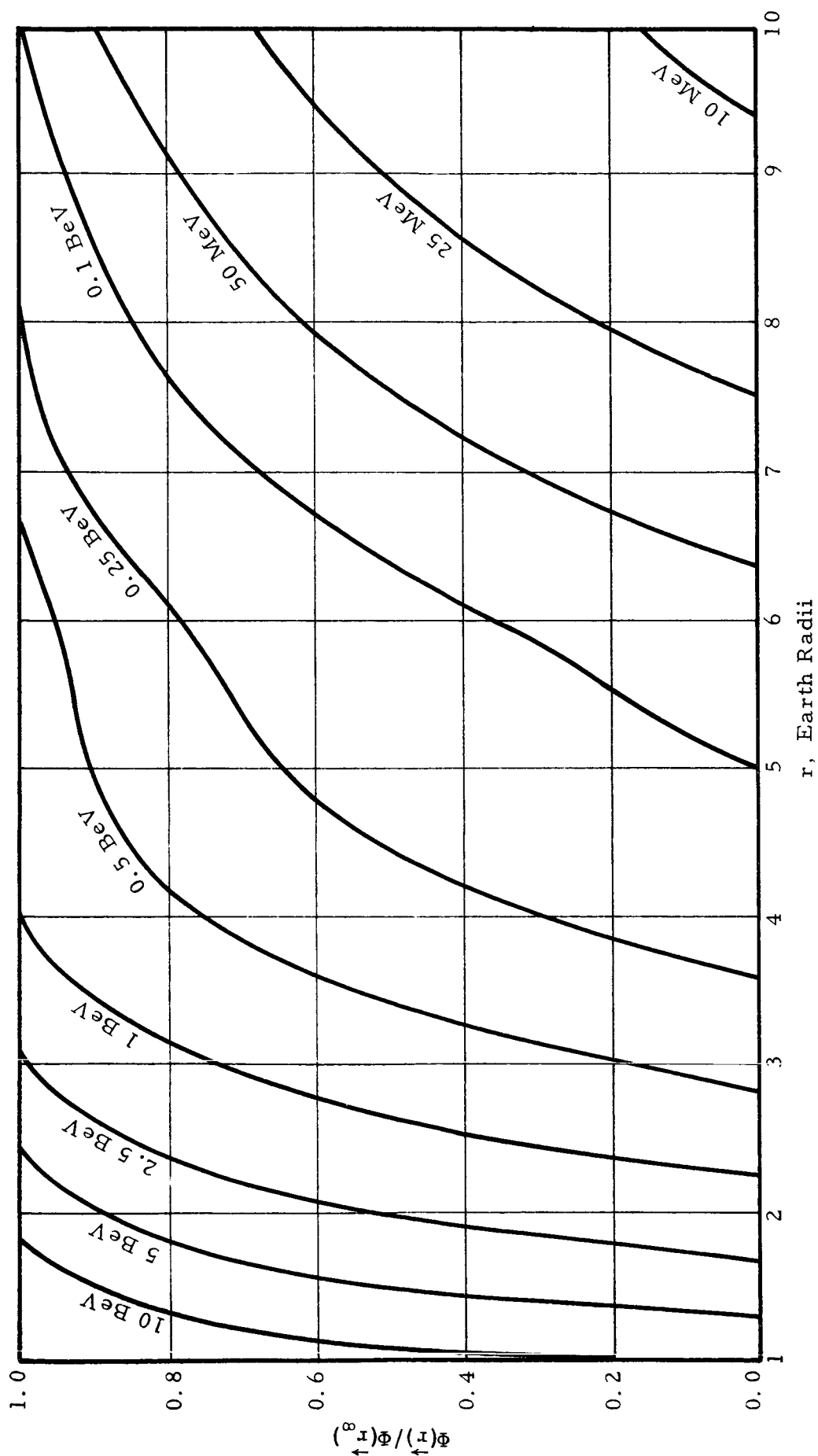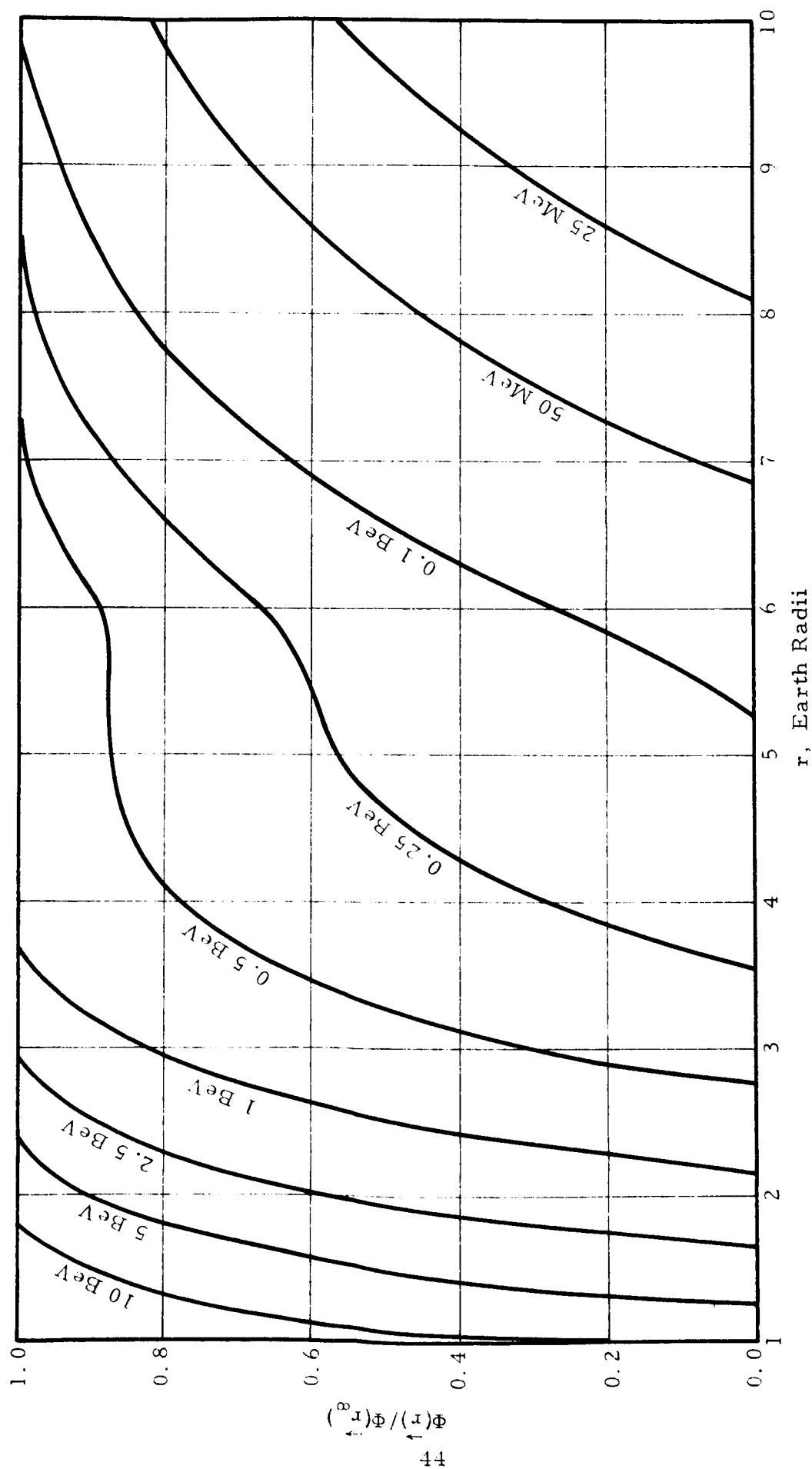
44

CONCLUSIONS

The Störmer theorem has been applied to the combination field of a dipole plus a distributed ring current. Forbidden regions for unbound particle motion were calculated and ratios of unbound proton flux in the model magnetosphere to an isotropic flux at infinity were obtained. These ratios indicate that the reduction of unbound particle flux near the ring current and outside it due to the presence of the ring may be of greater magnitude than the increase of particle flux at the Earth's surface due to the ring current.

The unbound charged particle distributions in the magnetosphere are strongly influenced by the presence of a ring current. The theoretical distributions appear to be rather sensitive to the form assumed for the ring current.

More accurate predictions of the effect of the ring current on the distribution of unbound particles in the magnetosphere may be obtained with more accurate representation of the vector potential of the ring current. A multiple-sheet representation for the ring current would be nearer to the diffuse nature of the actual trapped particle belts than the single sheet approximation used in these calculations. The multiple sheet formulation appears to be a straight-forward transition from the present formulations. For some range of particle energy, each added current sheet may have its own saddle point but it should not be too difficult to decide which pass points control the particle flux for each region of Störmer space. Very accurate representations of the ring current vector potential, especially those which are not axisymmetric and those obtained by numerical integration will very probably be too complicated for use with the Störmer theory and individual particle trajectories will probably have to be numerically integrated to determine allowed directions of arrival, cutoff rigidities and particle fluxes.

45

Satellite particle flux data should be analyzed for an experimental measure of the influence of the trapped particle belts on the untrapped particle flux. Maps of measured cutoff energy for free particles for the magnetosphere could be compared with the results of the Störmer theory using various ring current models. The measured untrapped particle distributions in the magnetosphere should be of considerable value in the study of the ring current.

The Störmer theory may serve as a useful check in efforts to derive self-consistent models of the ring current and its magnetic field. [27,28] The ring current effects on solar flare particles should be considered when predictions of the penetration of these particles into the magnetosphere are made. The magnitude of the ring current effect appears to be such that the flux of solar flare protons in the magnetosphere differs substantially from what might be expected in a dipole field.

REFERENCES

1. Schmidt, A., Z Geophys. 1, 1 (1924-25)

2. Chapman, S. and V. C. A. Ferraro, Terrestrial Magnetism and Atm. Elec. 37, 77 (1931); 36, 171 (1931); 37, 147 (1932); 37, 421 (1932; 38, 79 (1933)

3. Alfvén, H., Cosmic Electrodynamics, Oxford University Press, London, 1950

4. Treiman, S. B., "Effect of Equatorial Ring Current on Cosmic-Ray Intensity", Phys. Rev. 89, No. 1, pp. 130-133 (1953)

5. Ray, E. C., "Effects of a Ring Current on Cosmic Radiation", Phys. Rev. 101, No. 3, pp. 1142-1148, (1956)

6. Ray, E. C., "Effects of a Ring Current on Cosmic Radiation Impact Zones", Phys. Rev. 104, 5 (1956)

7. Akasofu, S.-I. and W. C. Lin, "The Magnetic Moment of Model Ring Current Belts and the Cutoff Rigidity of Solar Protons", Jour. Geophys. Res. 68, No. 4, pp. 973-977 (1963)

8. Akasofu, S.-I. and J. C. Cain, "The Magnetic Field of the Radiation Belts", NASA TN D-1762, 1963

9. Akasofu, S.-I. and J. C. Cain, "The Magnetic Field of the Quiet-Time Proton Belt", NASA TN D-1674, 1963

10. Akasofu, S.-I. and Sydney Chapman, "The Ring Current, Geomagnetic Disturbance, and the Van Allen Radiation Belts", Jour. Geophys. Res. 66, No. 5, pp. 1321-1350, 1961

11. Ben'kova, N. P. and L. O. Tyurmina, "Magnetic Field of the Equatorial Current", Geomagnetism and Aeronomy 2, No. 4, 1962, NASA TT F-8303, 1962

12. Chapman, Sydney, Solar Plasma, Geomagnetism and Aurora, Gordon and Breach, New York, 1964

13. Ray. E. C., "The Terrestrial Ring Current", Jour. Geophys. Res. 69, No. 21, pp. 4421-4427 (1964)

14. Smythe, W. R., Static and Dynamic Electricity, McGraw-Hill Book Company, Inc., New York, 1950

15. Gröbner, Wolfgang and Nikolaus Hofreiter, _Integraltafel, Erster Teil, Unbestimmte Integrale_, Springer Verlag, Wein, 1961

16. Stern, David, "The Vector Potential and Motion of Charged Particles in Axisymmetric Magnetic Fields", Jour. Geophys. Res. 69, No. 13 (1964)

17. Störmer, Carl, _The Polar Aurora_, Oxford University Press, London, 1955

18. Vallarta, M. S., "Theory of the Geomagnetic Effects of Cosmic Radiation", _Handbuck der Physik_, Bd XLVI, Springer-Verlag, Berlin, 1961

19. Johnson, T. H., "Cosmic-Ray Intensity and Geomagnetic Effects", Rev. Mod. Phys. 10 (1938)

20. Urban, E. W., "Charged Particle Motion in Axially Symmetric Magnetic Fields", Masters Thesis, University of Alabama, 1963

21. Urban, E. W., "Critical Störmer Conditions in Quadrupole and Double Ring Current Fields", Jour. Math. Phys. 6, No. 12, pp. 1966-1975 (1965)

22. Prescott, A. D., "Distribution of Unbound Charged Particles in the Static Magnetic Field of a Dipole", NASA TM X-51312, N64-17685, 1964

23. Prescott, A. D., "Some Fundamental Characteristics of Charged Particle Motion in Axially Symmetric Multipole Fields", MSFC, R-RP-INN-65-1, February, 1965

24. Swann, W. F. G., "Application of Liouville's Theorem to Electron Orbits in the Earth's Magnetic Field", Phys. Rev. 44, pp. 224-227 (1933)

25. Prescott, A. D., Urban, E. W. and R. D. Shelton, "The Application of the Liouville Theorem to Magnetic Shielding Problems", Second Symposium on Protection Against Radiation in Space, NASA SP-71, pp. 189-198 (1964)

26. Ray, E. C., "On the Application of Liouville's Theorem to the Intensity of Radiation Trapped in the Geomagnetic Field", State University of Iowa, SUI-59-21, 1959

27.   Beard, D. B., "Self-Consistent Calculation of the Ring Current",
       Jour. Geophys. Res. 67, No. 9, p. 3615 (1962)

28.   Akasofu, S. -I., "On a Self-Consistent Calculation of the Ring Current
       Field", Jour. Geophys. Res. 67, No. 9, p. 3617 (1962)

DOCUMENT CONTROL DATA · R&D

(Security classification of title, body of abstract and indexing annotation must be entered when the overall report is classified)

1. ORIGINATING ACTIVITY (Corporate author)	2a. REPORT SECURITY CLASSIFICATION
Research Laboratories Brown Engineering Company, Inc. Huntsville, Alabama	Unclassified
	2b. GROUP N/A

3. REPORT TITLE

"Effect of the Ring Current on the Distribution of Unbound Particles in the Magnetosphere"

4. DESCRIPTIVE NOTES *(Type of report and inclusive dates)*

Technical Note, June 1966

5. AUTHOR(S) *(Last name, first name, initial)*

McDonald, Perry F.

6. REPORT DATE	7a. TOTAL NO. OF PAGES	7b. NO. OF REFS
June 1966	61	28

8a. CONTRACT OR GRANT NO. NAS8-20166	9a. ORIGINATOR'S REPORT NUMBER(S)
b. PROJECT NO. N/A	TN R-204
c.	9b. OTHER REPORT NO(S) (Any other numbers that may be assigned this report) None
d.	

10. AVAILABILITY/LIMITATION NOTICES

None

11. SUPPLEMENTARY NOTES	12. SPONSORING MILITARY ACTIVITY
None	Research Projects Laboratory George C. Marshall Space Flight Center NASA

13. ABSTRACT

The effect of the ring current due to the drift of trapped particles in the radiation belts on the distribution of untrapped particles in the magnetosphere is analyzed using a current sheet approximation to the ring current. The shape assumed for the current sheet is the figure obtained by rotating a dipole field line about the axis. The vector potential of a dipole plus a distributed ring current is derived and applied in Störmer's theorem to determine allowed and forbidden regions of particle motion. Liouville's theorem is used to obtain the ratio of unbound particle flux at points inside the model magnetosphere to an isotropic uniform flux at infinity.

14. KEY WORDS

- ring current
- untrapped particles
- magnetosphere
- cosmic rays
- solar proton flux
- radiation belts
- Störmer's theorem
- Liouville's theorem